




Revision of the genus *Neptis* Fabricius, 1807 (Papilionoidea: Lepidoptera: Nymphalidae) in the Afrotropical Region, Part 4: The phylogeny of the Nysiades group with eight new species

Published online: 31 December 2022

urn:lsid:zoobank.org:pub:7CF9077A-E55B-4290-8EFA-A47448254139

DOI: <https://dx.doi.org/10.4314/met.v33i1.15>

Kwaku Aduse-Poku¹  Email: kadusepoku@gsu.edu; David J. Lohman²  Email: dlohman@ccny.cuny.edu; Ian D. Richardson*³  Email: ian.richardson.fr@gmail.com.

¹ Georgia State University, Perimeter College, Life, Earth Sciences Department, 3251 Panthersville Rd, Decatur, GA 30034, USA.

² City College of New York, City University of New York, 160 Convent Ave, New York, NY 10031, USA; Graduate Center, City University of New York, 365 5th Ave, New York, NY 10016, USA; Entomology Section, National Museum of Natural History, Manila 1000, Philippines.

³ 23 Ridgewood Drive, Burton-upon-Stather, Lincolnshire, DN15 9YE, UK. * = corresponding author.

Copyright © Lepidopterists' Society of Africa, and the authors.

Abstract: A multigene phylogenetic hypothesis is presented for the Nysiades group of Afrotropical *Neptis* species. The tree shows evolutionary relationships among the 24 currently described species in the group and eight additional new species that are formally described here. The eight new species are assigned to three subgroups within the Nysiades group based on evidence of their evolutionary affinities. Multiple specimens of each of the novel species have been barcoded, K2P pairwise genetic distances among these new species further support their status.

Key words: DNA barcodes, genitalia, Limenitidinae

Citation: Aduse-Poku, K., Lohman, D.J. & Richardson, I.D. 2022. Revision of the genus *Neptis* Fabricius, 1807 (Papilionoidea: Lepidoptera: Nymphalidae) in the Afrotropical Region, Part 4: The phylogeny of the Nysiades group with eight new species. *Metamorphosis* 33: 130–163.

Peer reviewed

INTRODUCTION

The Nysiades Group

Richardson (2019) presented a phylogeny of Afrotropical *Neptis* species that includes a large clade of forest-associated species that was named the Nysiades group after its oldest species, *Neptis nysiades* Hewitson, 1868. The phylogeny is derived from DNA barcodes and bootstrap support for many nodes is low, suggesting that relationships within the group are unreliable. The Nysiades group clade comprised 30 described species and a further 45 putative undescribed species (Richardson, 2019).

Members of the Nysiades group can be recognised, in most cases, by the following combination of characters:

- the absence of patches of dark shading on the submarginal lines in spaces M3 and R5 (Fig. 1 red arrow)
- the basal lines on the hindwing underside, hb2 and hb3 using the notation introduced in Richardson (2019) well separated and continuous (Fig. 1 yellow arrows)
- the valve of the male genitalia terminating, posteriad, in a linear process with a rounded end and one or two hooks in many instances (Fig. 2), but note *N. ginettae* sp. nov. is an exception
- the area around the ostium bursae is not sclerotised in the female.

Received: 12 October 2022

Accepted: 15 December 2022

This work is licensed under a Creative Commons Attribution-NonCommercial-NoDerivs 4.0 International License. To view a copy of this license visit:

<http://creativecommons.org/licenses/by-nc-nd/4.0/>

Multigene phylogeny

A comprehensive phylogenetic study of the genus *Neptis* is being undertaken by the first two authors to expand upon the work of Ma *et al.*, (2020). Published and unpublished analyses demonstrate that all African *Neptis* are a monophyletic group descended from an ancestor that dispersed to Africa from Asia. Unlike the tree based on

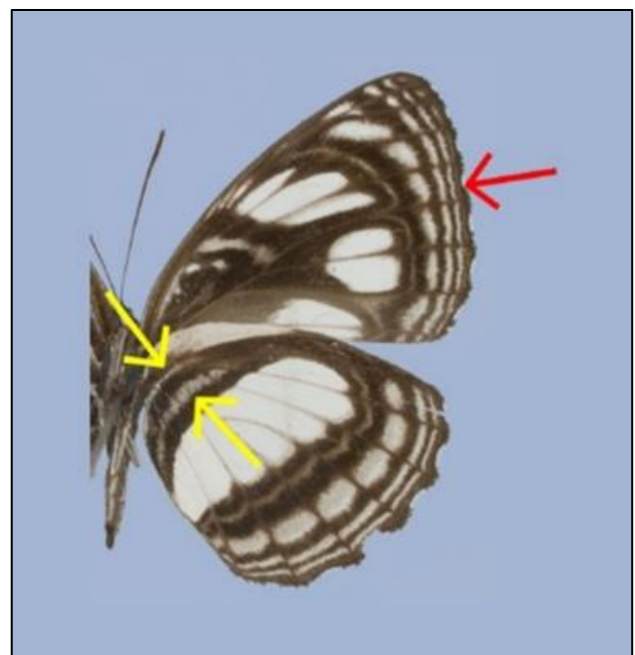


Figure 1 – The underside of *Neptis stellata* Pierre Baltus & Pierre, 2007 showing absence of shading on forewing submarginal bands, red arrow, and continuous well separated basal lines hb2 and hb3 on hindwing.

DNA barcodes, the multigene phylogeny presented here for Afrotropical *Neptis* species in the Nysiades group has high bootstrap support, indicating strong evidence for the inferred relationships among species.

This multigene tree expands the Nysiades group to include *Neptis seeldrayersi* Aurivillius, 1895, *Neptis alta* Overlaet, 1955 and *Neptis collinsi* Richardson, 2020. It is reasonable to infer that *Neptis rogersi* Eltringham, 1921 is in this wider Nysiades group as both barcode and facies show it to be closely related to *N. collinsi*. The latter two species inhabit forest patches on the East African coast and Mt. Mabu in Mozambique, and *Neptis seeldrayersi* is also a forest species. *Neptis alta* is unusual for the Nysiades group because it inhabits both the main forest belt and woodland habitats far from the forest.

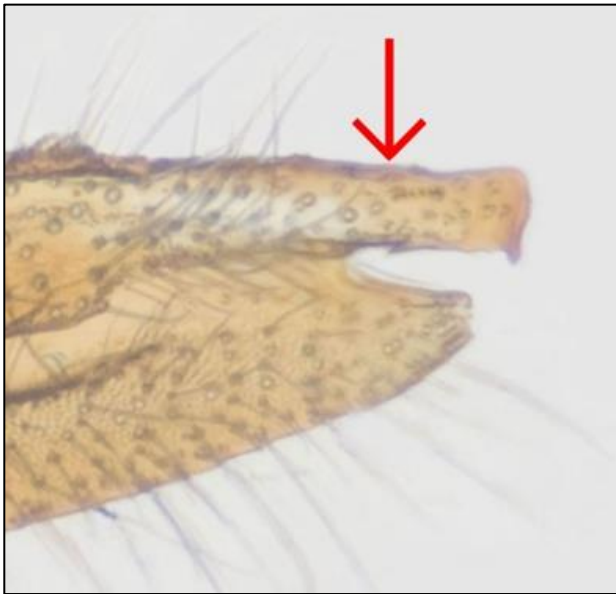


Figure 2 – The posterior extremity of the valve of *Neptis kupe* sp. nov. showing the linear apical process, arrowed, with a slightly rounded end and a single ventral hook.

The inventory for the Nysiades group, following the current paper, stands at a total of 40 described species of which 28 are sampled in the multigene tree. A continuing barcoding exercise has revealed an additional 40 new species to be critically examined and described.

The new species were given provisional names in the format speciesNNN (where NNN runs from 1 to 101) in Richardson (2019) and are here assigned to the following taxa and subgroups within the Nysiades group:

- Kupe subgroup
 - *Neptis kupe* sp. nov. (species61)
 - *Neptis jamesi* sp. nov. (species31)
 - *Neptis nanciae* sp. nov. (species33)
- Metanira subgroup
 - *Neptis metanira* Holland, 1892
 - *Neptis ducarmei* sp. nov. (species2)
 - *Neptis ginettae* sp. nov. (species3)
 - *Neptis sobrina* sp. nov. (species9)
- Lugubris subgroup
 - *Neptis lugubris* Rebel 1914
 - *Neptis angelae* sp. nov. (species39)
 - *Neptis paulinae* sp. nov. (species92)

The Metanira subgroup is named after the existing taxon *Neptis metanira* and the Lugubris subgroup is named after the existing taxon, *Neptis lugubris*. There is no existing taxon in the first subgroup, hence we selected a representative species in the subgroup as the subgroup name.

MATERIALS AND METHODS

Molecular methods

Twenty-eight specimens representing two-thirds of all described Nysiades group species and eight novel taxa comprised the ingroup sample, and five Asian *Neptis* species were included as outgroups. Samples were either collected by the authors during field expeditions or donated by collaborators. For samples that were freshly ethanol-preserved in the field, we extracted genomic DNA from one or two leg(s). For older museum material or dried specimens, we extracted DNA from thoracic tissues. Genomic DNA was extracted using an OmniPrep™ Genomic DNA Purification Kit, following a modification of the manufacturer's suggested protocol. Thirteen molecular markers were amplified and sequenced via anchored hybrid enrichment using the probe set of Kawahara *et al.* (2018) which includes one mitochondrial locus (cytochrome c oxidase subunit I, COI) and twelve nuclear: acetoacetyl-CoA thiolase, AACT; carbamoylphosphate synthetase domain protein, CAD; Catalase, CAT; dopa-decarboxylase, DDC; elongation factor 1 alpha, EF-1 α ; glyceraldehyde-3-phosphate dehydrogenase, GAPDH; Hairy cell leukemia protein 1, HCL; isocitrate dehydrogenase, IDH; cytosolic malate dehydrogenase, MDH; ribosomal protein S2, RpS2; ribosomal protein S5, RpS5; and wingless, wg. Bioinformatic workflow followed Breinholt *et al.* (2018). Nucleotide sequences were aligned by eye using Bioedit v7.2.5 (Hall, 1999). The software MEGA v7.0.14 (Tamura *et al.*, 2013) was used to assess potential errors such as stop codons and contamination. The cleaned sequences were then concatenated with SequenceMatrix 1.9 (Vaidya *et al.* 2011) to produce a final matrix of 33 taxa and 14,351 aligned nucleotides.

All characters were equally weighted and gaps were treated as missing data. Phylogenetic inferences were made using a Maximum Likelihood (ML) approach implemented in IQ-TREE 2.2.0 (Minh *et al.*, 2020). The best-fit partitioning scheme and models of nucleotide substitution were estimated simultaneously using the greedy algorithm in MODELFINDER (Kalyaanamoorthy *et al.*, 2017), with the optimal models chosen based on corrected Akaike Information Criterion (AICc). The best-fit models of nucleotide substitution were determined across all available models in IQ-TREE, including the FreeRate model (+R; Soubrier *et al.*, 2012), which relaxes the assumption of gamma distributed rates. We assessed nodal support of recovered relationships using 1000 generated replicates for ultra-fast bootstraps, UFboot (Hoang *et al.*, 2018) and Shimodaira–Hasegawa approximate likelihood ratio test, SH-aLRT (Guindon *et al.*, 2010). To overcome model violations inherent in UFBoot calculations, the '-bnni' command was added to improve the search for each UFBoot replicate tree. When discussing branch support of

clades, nodes recovered with SH-aLRT ≥ 85 and UFBoot ≥ 95 are considered strongly supported.

Notation

The notation for wing markings in the *Neptis* introduced in Richardson (2019) is used in the sections ‘Description of the facies’ and ‘Diagnosis’.

Specimen photography

Dorsal and ventral aspects of all specimens for DNA sequencing were photographed using the technique described in Richardson (2019). A scale bar is provided on each set of specimen images.

The accession numbers of photographed specimens are stated in the figure captions and a shortened version of the ABRI accession number is used. For example, ABRI-2018-1234 becomes ABRI-181234.

Acquisition of barcodes for genetic pairwise distance analyses

A single leg was removed from each barcoded specimen and submitted to the Canadian Centre for DNA Barcoding, Guelph, Canada, along with an image of the dorsal and ventral view of the set specimen. The samples were sequenced to yield the barcode COI.

A Klee diagram was constructed using K2P corrected pairwise distances (PD) between the barcodes of each described and undescribed species. The diagram comprises a list of samples written top to bottom on the left-hand side and an identical list written left to right across the top. This is illustrated for a simple case in Fig. 3 for specimens of two closely related species, *N. stellata* Pierre Baltus & Pierre, 2007 and *N. nigra* Pierre Baltus & Pierre, 2007. The PD for each pair of specimens, one from the left-hand column and one from the top row, is written at the intersection forming a PD matrix. Only the lower left half of the matrix is shown, as the upper right half is simply a mirror image along the diagonal.

	Country	DRC	DRC	DRC	DRC	DRC	DRC	DRC	DRC
Country	Species	<i>stellata</i>	<i>stellata</i>	<i>stellata</i>	<i>stellata</i>	<i>nigra</i>	<i>nigra</i>	<i>nigra</i>	<i>nigra</i>
DRC	<i>stellata</i>								
DRC	<i>stellata</i>	0.0							
DRC	<i>stellata</i>	0.0	0.0						
DRC	<i>stellata</i>	0.2	0.2	0.2					
DRC	<i>nigra</i>	3.0	3.0	3.0	2.8				
DRC	<i>nigra</i>	3.1	3.1	3.1	2.9	0.0			
DRC	<i>nigra</i>	3.0	3.0	3.0	2.8	0.0	0.0		
DRC	<i>nigra</i>	3.0	3.0	3.0	2.8	0.0	0.0	0.0	

Figure 3 – An example of a Klee diagram for specimens of *Neptis stellata* and *Neptis nigra* Pierre Baltus & Pierre, 2007

For easier visual assessment, the cells are colour-coded from red, PD = 0%, through yellow, green, blue to black for increasing PD. When conspecific samples are grouped, well-separated species form red triangles to the left and below the diagonal with zones of higher PD between.

In Fig. 3, the two species triangles are separated by a relatively high PD = 3% zone.

Genitalic dissection

The techniques employed to dissect and photograph the genitalia of male specimens and the sternites and tergites of female specimens are described in Richardson (2019). Note that the internal organs of the females are not distinctive in *Neptis*; only the form of the sternites and tergites may be diagnostic.

All the images of genitalia are shown with a 1 mm scale bar.

Distribution Map

A map of Africa covering the localities for the new species was developed from the website <https://maps-for-free.com>. The map shows elevation, principal rivers/lakes, and international boundaries. The map is used as the basis for an Excel chart in a workbook with formulae to transform specimen capture latitude and longitude to the map coordinates.

Different symbols are used for each species. The symbol border and fill indicate the status of the specimen as follows:

- Holotype: red fill
- Paratype: yellow fill
- Other specimens: white fill
- Barcoded specimens: black outline
- Specimens not barcoded: pale blue outline

RESULTS

Multi-gene phylogenetic tree

The inferred phylogenetic tree confirmed the Nysiades group to be monophyletic (Fig. 4). The 8 new species were recovered as three distinct subgroups within Nysiades. *Neptis paulinae* sp. nov. and *N. angelae* sp. nov. were recovered with *N. lugubris* Rebel, 1914, with variable support (SH-aLRT=100; UFBoot=45), constituting the *Lugubris* subgroup. Similarly, *N. sobrina* sp. nov., *N. ducarmei* sp. nov. and *N. ginette* sp. nov. formed a well-supported clade with the described species *N. metanira* as their closest sister taxon (SH-aLRT=100; UFBoot=72). The clade is henceforth called the *Metanira* subgroup. The remaining new species, *N. nanciae* sp. nov., *N. kupe* sp. nov. and *N. jamesi* sp. nov. were recovered as a well-supported clade sharing a more recent ancestor with four described species including the widely distributed forest species *N. strigata* Aurivillius, 1894, and *N. conspicia* Neave, 1904, (Fig. 4).

Klee diagram

The Klee diagram, Fig. 5, shows the barcode K2P corrected PD matrix for a selection of specimens of the Nysiades group specimens that have been barcoded. For simplicity, the PD value is not written to each cell, but an approximation of the PD values is indicated by the cell colour. The specimen data column to the left and row at the top are not shown. The red triangles are intraspecific comparisons, and each species' triangle is labelled.

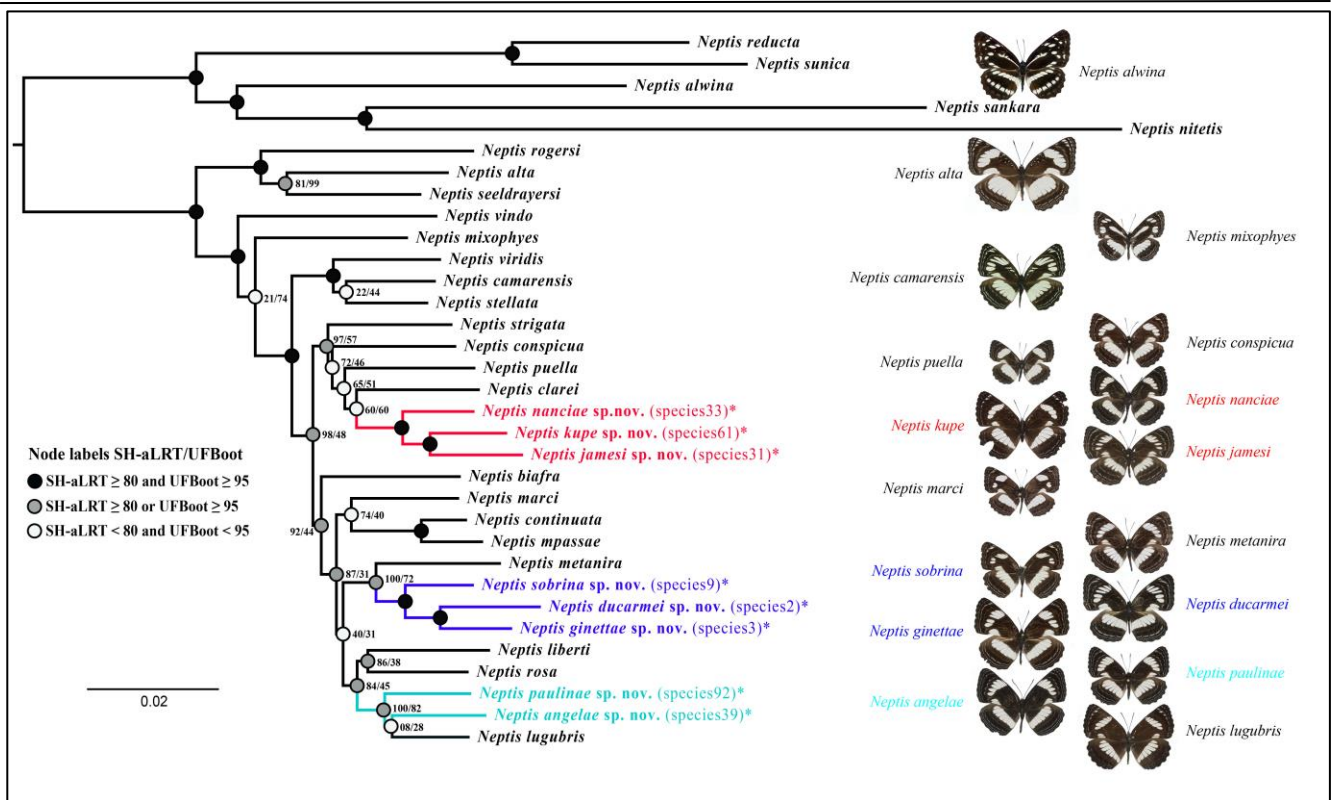


Figure 4 – The phylogeny of the Nysiades group of Afrotropical species in the genus *Neptis*

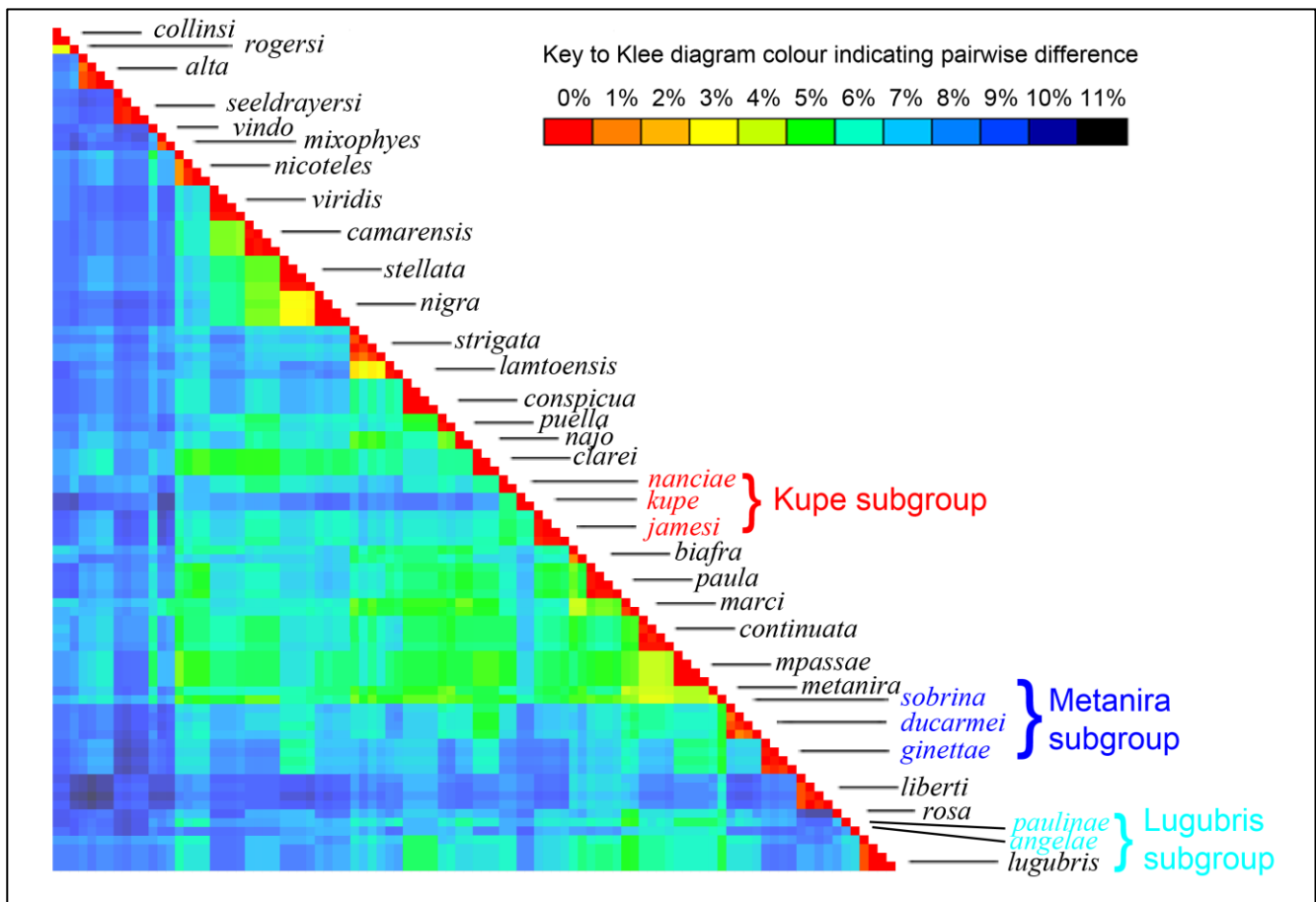


Figure 5 – Klee diagram showing barcode pairwise differences within the Nysiades group of the *Neptis* genus. The names of the new species are coloured as in the multigene phylogeny and species subgroup names are shown in same colours.

Species are well separated by zones of high PD, strongly supporting their monophyly. The lowest PD between species is approximately 3%, as shown by the yellow

zones. All new species described below form isolated, low PD triangles separated from one another and other species by at least 5%, indicating strongly differentiated species.

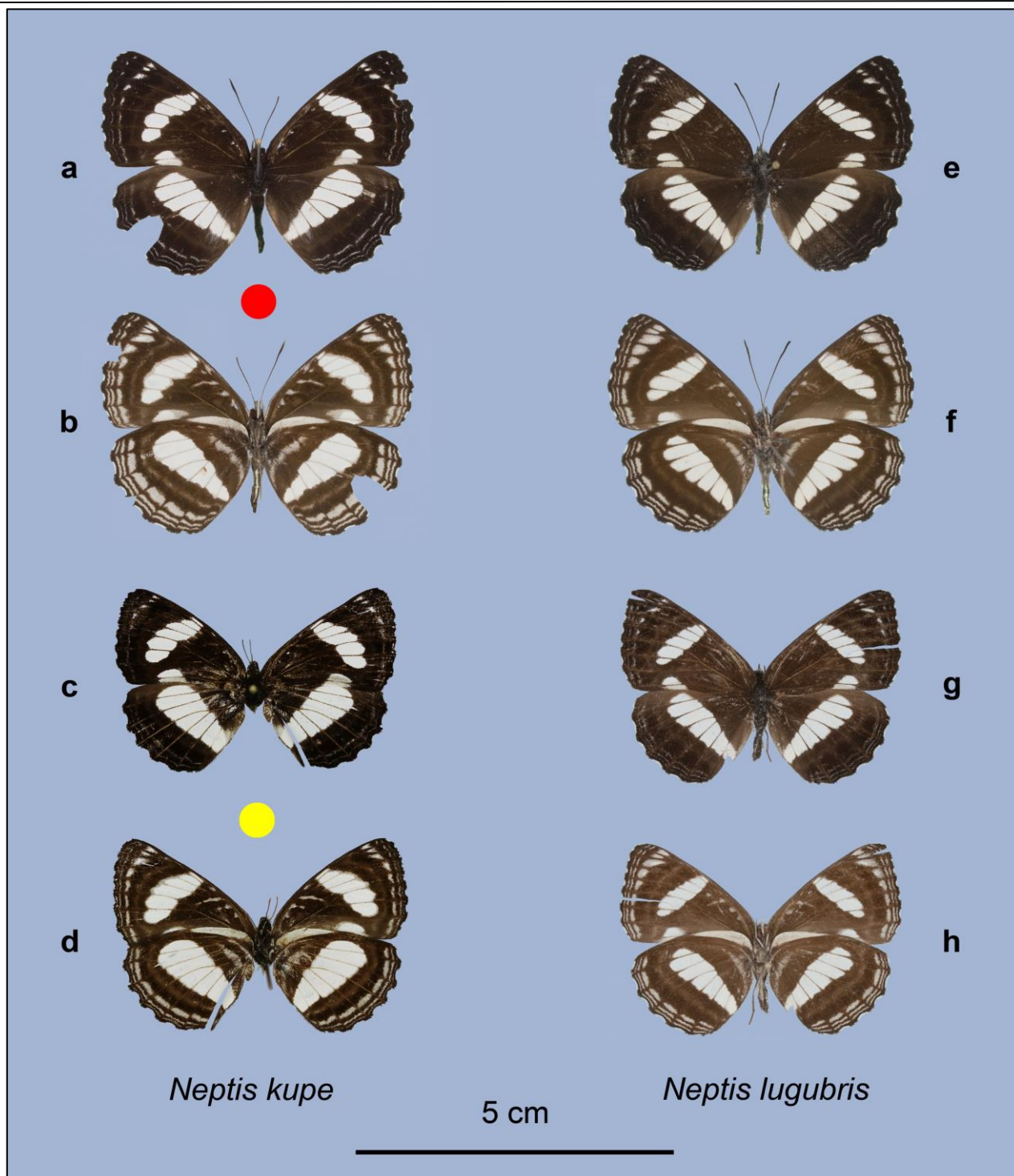


Figure 6 – *Neptis kupe* sp. nov. compared with *Neptis lugubris* Rebel, 1914. *N. kupe* holotype ♂: ABRI-152668, Mt Kupe, Cameroon, iv.2014, **a** dorsal, **b** ventral; *N. kupe* paratype ♀: ANHRTUK00214938, Mt Kupe, Cameroon, 23.i.2012, R. Tropek, **c** dorsal, **d** ventral; *N. lugubris* ♂: ABRI-152640, Biakato, DRC, v.2011, **e** dorsal, **f** ventral; *N. lugubris* ♀: ABRI-152648, Kibale, DRC, vi.2013, **g** dorsal, **h** ventral.

DESCRIPTIONS OF NEW SPECIES

Genus *Neptis* Fabricius, 1807

Illiger, K., *Magazin für Insektenkunde* 6: 282 (277–289).

Type-species: *Papilio aceris* Esper, by subsequent designation (Crotch, 1872). *Cistula Entomologica* 1: 66 (59–71).

Kupe subgroup

Neptis kupe sp. nov. (Fig. 6)

urn:lsid:zoobank.org:act:89E58A84-519B-4E2D-AC5B-026DFB151772

In January 2012, Robert Tropek undertook a collecting expedition to Mount Kupe (Koupé) in West Cameroon and captured a specimen with facies similar to those of *Neptis lugubris* Rebel 1914. This expedition was followed up in April the next year by Szabolcs Sáfíán, Robert Tropek, and Marianne Espeland who captured further specimens of this *N. lugubris*-like species. An ABRI-commissioned collector captured a further specimen the following year. Subsequent molecular analysis showed that the Mt. Kupe specimens are distinct from *N. lugubris*, and these are described here as *Neptis kupe* sp. nov. It will be shown that these two species can also be separated by the facies.

Holotype: ♂ Mt. Kupe, Cameroon, 04°48' N, 09°42' E, 1500–1900 m, iv.2014; ABRI-152668, ABRI collector.

Paratypes: ♂ same locality, 7–10.iv.2014, Sáfián, Tropek, Espeland, ANHRTUK00214937, ANHRT collection; ♀: same locality, i.2012, Tropek, ANHRTUK00214938, ANHRT collection; 1 unknown sex: same locality, 7–10.iv.2014, Sáfián, Tropek, Espeland, ABRI-152667, ABRI collection.

Description of facies

Holotype: ♂ ABRI-152668 (Fig. 6 a, b)

Wingspan: 4.9 cm. **Forewing length:** 2.8 cm. **Antenna-wing ratio:** 0.43.

Head: Dark brown and unmarked; palps light grey; antennae upperside dark grey along the entire length, antennae underside dark grey with more reddish brown tip.

Thorax: Upperside dark grey, underside dark brown. Legs, brown distally.

Abdomen: Upperside almost black, broadly grey on underside with traces of lighter lateral line, well-defined continuous whitish ventral line.

Wings: Forewing upperside: Background colour dark brown grading to lighter shade of brown towards root. Cell unmarked, three short pale-brown radial lines beyond distal end close to costa. Discal band markings white. Long discal band mark in space 2A (fd1) tapering progressively distad and more sharply proximad, mark in space Cu2 (fd2) shorter than fd1 and tapering in same way, broadly separated (2 mm) by background colour from mark in space Cu1 (fd3). Marks in spaces Cu1 to R5 (fd3 to fd7) forming irregular band convex distad and slightly concave proximad, marks being separated narrowly by background colour along veins. Discal band marks longest in M2 and M1 (fd5 and fd6) then shorter in R5 (fd7). Marks fd4 and fd5 shaped proximad to form notch. Narrow, elongated mark in R3 (fd8), this mark more broadly separated than other marks in discal band. Post discal band missing. Two submarginal bands, inner band (fsm1) comprising faint linear marks slightly convex proximad from space Cu2 to M3, then marks broadening towards the apex in spaces M2 to R3, mark in space R4 the largest. Outer submarginal band (fsm2) lightly marked, and crescent shaped in spaces Cu2 to M2, convex proximad, remainder of band to apex in spaces M1 to R3 comprising faint white spots. Outer margin with black cilia, indented at veins with narrow patch of white cilia. **Forewing underside:** Ground colour chocolate brown much lighter than upperside, markings white and in same pattern as upperside but more distinct. Cell markings comprising radial bar at base (fcr) terminating in small white spot surrounded by pale brown area. fcr separated by ground colour from fct1, which comprises small spot again surrounded by pale brown extending to short transverse line. fct1 separated from distal transverse line fct2 by ground colour, fct2 pale brown and extending across $\frac{3}{4}$ of cell width. Four pale brown radial lines beyond end of cell in spaces Sc, R1, R2 and R5, latter shorter than other three. Discal band as upperside but with pale brown shading distad and proximad, the shading extensive on proximal side of fd2. Postdiscal line faintly marked lighter than background and extending from inner margin almost to costa, band indented proximad in space Cu2. Three submarginal bands clearly marked. Proximal band (fsm1) comprising pale brown linear marks in spaces

2A to M2, then becoming more pointed proximad towards apex, mark in R5 longest. Band fsm2 extending from space 2A to space R3 and comprising pale brown arcs convex proximad. Distal band fsm3 similar but not present in space 2A. **Hindwing upperside:** Unmarked at base. Broad white discal band (hd) extending from inner margin in space 2A to space Rs, narrow at inner margin and broadening to hd6 in space M1, and ending with shorter mark rounded on anterior edge in space Rs, all marks narrowly separated by ground colour at veins and flat ended distally. Postdiscal line faintly marked fuzzy lighter brown. Three narrow pale brown submarginal bands, proximal band (hsm1) comprising near linear marks, hsm2 and hsm3 comprising curved lines convex proximally in each space. All three submarginal bands faintly marked darker brown at inner margin and towards the costa. Outer margin scalloped as forewing, but with broader patches of white cilia. **Hindwing underside:** Basal line along costa (hb1) brownish white and extending along approximately 45% of length of costa, second basal line (hb2) pale brown, weakly defined at inner margin followed by two faint detached spots distad, third basal line (hb3) pale brown, well defined from inner margin to space M2, with detached spot in M1. Discal band white as on upperside and with traces of pale brown shading on distal edge in spaces M2 and M1. Postdiscal band extending from inner margin and curving around discal band to space Rs, more reddish brown than background colour and dusted with lighter scales particularly in space Cu2. Three submarginal bands comprising of white marks well separated at veins. Proximal band (hsm1) broad, narrowing at extremities, extending from inner margin to space Rs. Middle band (hsm2) narrow and comprising slightly curved marks convex proximad, extending from inner margin to space Rs. Third band (hsm3) similar and extending from space Cu2 to space Rs.

Genitalia: ♂ (Fig. 7) Uncus curving uniformly ventrad with a hooked tip. Ventral edge of valve curved, dorsal edge straight from apical process along $\frac{3}{4}$ of length of valve, aspect ratio height/length = 0.26, apical process comprising a straight stem terminating in a ventral hook turning proximad, ventral closure narrow and coming to a point, dorsal process an elongated triangular shape. Aedeagus short and broad, length ratio relative to the valve, A/V = 0.86.

Paratype: ♀ ANHRTUK00214938 (Fig. 6 c, d): Mt. Kupe, Cameroon, 04°48' N, 09°42' E, (4.8000°, 9.7000°), 1500–1900 m, iv.2014, ABRI collection.

The description below highlights the differences between the holotype and the paratype rather than repeating elements that are almost identical.

Head: Same as holotype.

Thorax: Same as holotype.

Abdomen: Same as holotype except thin ventral line more clearly defined.

Wings: Forewing upperside: Discal band broader at fd3 and fd4, submarginal band fsm1 less clearly marked and almost obsolete from cell 2A to cell M2. **Forewing underside:** Cell mark fct represented by a second spot adjacent to fcr1. **Hindwing upperside:** Discal band broader particularly approaching the inner margin,

submarginal bands very faint. **Hindwing underside:** Basal line hb2 narrow and clearly marked.

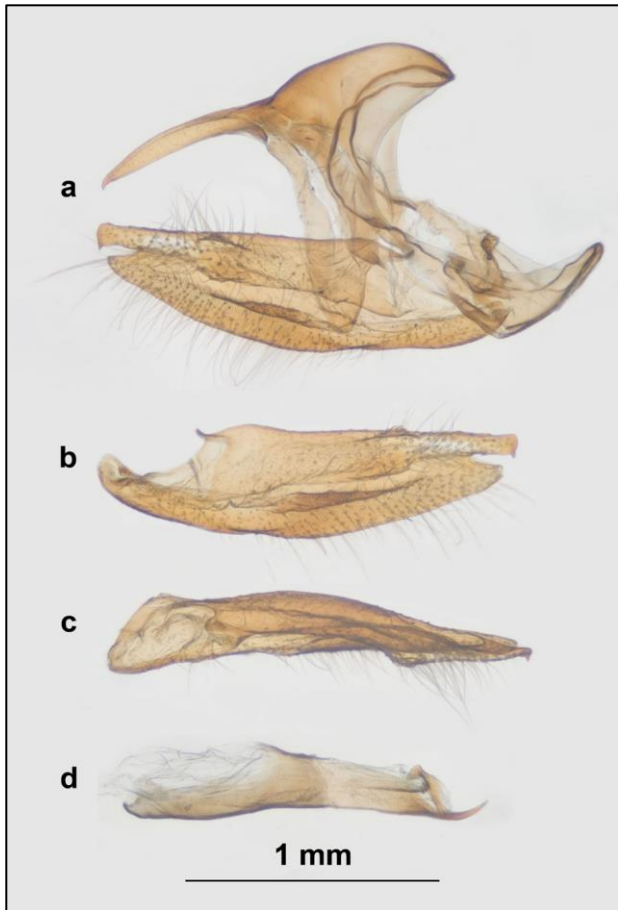


Figure 7 – Genitalia of *Neptis kupe* ♂: **a** lateral view of genitalia, **b** lateral view of valve, **c** dorsal view of valve, **d** lateral view of aedeagus. NHRTUK00214937, Mt Kupe, Cameroon, 7–10.iv.2013; S. Sáfián, R. Tropek, M. Espeland.

Sclerotisation of the abdominal exoskeleton: ♀ Ostium plate not sclerotised except for a broad band extending round anterior edge of ostium bursae, not closed on posterior edge. A pocket between the 7th and 8th tergites and the 8th tergite with notch on ventral edge.

The dissected exoskeleton was tightly curved and could not be flattened for photography without risk of damage.

Holotype barcode: 658 base pairs,

AACTTTATATTTTATTTTGGAAATCTGAGCTGGAAT
 AGTTGGAACATCTCTTAGTTTATTGATCCGAACTGA
 ATTAGGTAATCCAGGGTCTTTAATTGGAGATGATCA
 AATTTATAATACTATCGTAACTGCTCATGCATTTATT
 ATAATTTTTTTCATAGTTATACCTATTATAAATTGGGG
 GATTTGGCAATTGATTAATTCCTCTAATATTAGGAG
 CCCCTGACATAGCTTTCCCCCGAATAAATAATATAA
 GATTTTGATTACTCCCCCTTCTTTAATTTTATTAAT
 TTCTAGTAGAATTGTAGAACTGGGGCTGGAACAG
 GATGAACAGTATACCCCCCTATCTTCTAATATTG
 CTCATAGTGAGCTTCCGTAGATTTAGCTATTTTTC
 TTTACATTTAGCAGGTATTTCTTCTATTTTAGGAGCA
 ATTAATTTTATTACAATATTATTAACATACGTATTA
 ATAATATATCATTTGATCAAATACCTTTATTTGTTTG

ATCAGTGGGAATCACAGCTTTATTACTACTTTTATC
 TTTGCCTGTATTAGCAGGAGCTATTACAATATTATT
 AACAGATCGAAATTTAAATACTTCATTTTTTGATCC
 TGCTGGAGGAGGAGACCCTATTCTTTACCAACATTT
 ATTT

Barcoding

Two specimens of *N. kupe* yielded identical full-length barcodes, 658 base pairs, that are allocated to BOLD BIN: ACU3559. The nearest neighbours to *N. kupe* are the two new species described below, *N. jamesi* and *N. nanciae*, but several other species have slightly larger pairwise differences with *N. kupe*. The PDs between barcodes from the three species are shown in the Klee diagram, Fig. 8.

	Country	DRC	DRC	Cameroon	Cameroon	DRC	DRC	DRC	DRC	DRC	DRC
Country	Species	<i>nanciae</i>	<i>nanciae</i>	<i>kupe</i>	<i>kupe</i>	<i>jamesi</i>	<i>jamesi</i>	<i>jamesi</i>	<i>jamesi</i>	<i>jamesi</i>	<i>jamesi</i>
DRC	<i>nanciae</i>	0.0									
DRC	<i>nanciae</i>	0.0									
Cameroon	<i>kupe</i>	5.6	5.6	0.0							
Cameroon	<i>kupe</i>	5.6	5.6	0.0							
DRC	<i>jamesi</i>	5.6	5.6	5.9	5.9	0.2					
DRC	<i>jamesi</i>	5.4	5.4	5.8	5.8	0.2	0.0				
DRC	<i>jamesi</i>	5.4	5.4	5.8	5.8	0.2	0.0	0.2			
DRC	<i>jamesi</i>	5.2	5.2	5.9	5.9	0.3	0.2	0.2	0.2		
DRC	<i>jamesi</i>	5.5	5.5	5.8	5.8	0.2	0.0	0.0	0.0	0.2	
DRC	<i>jamesi</i>	5.4	5.4	5.8	5.8	0.2	0.0	0.0	0.2	0.0	0.0

Figure 8 – Klee diagram showing barcode pairwise differences, as percentages of the barcode length, between specimens of *Neptis kupe*, *Neptis jamesi* and *Neptis nanciae*.

Material examined and distribution

Four specimens of *N. kupe*, all from Mt. Kupe, have been examined as shown in Table 1. Three specimens of a separate population from Tabenken, further North in Cameroon, are also included. The collection localities of the *N. kupe* specimens and the Tabenken population in Cameroon are shown on the map, Fig. 9, along with

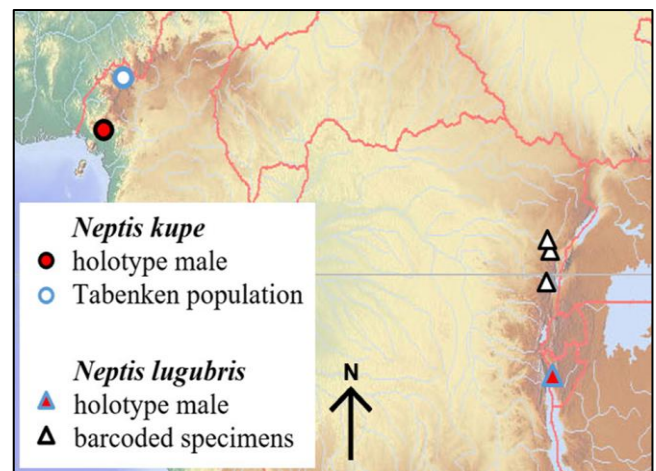
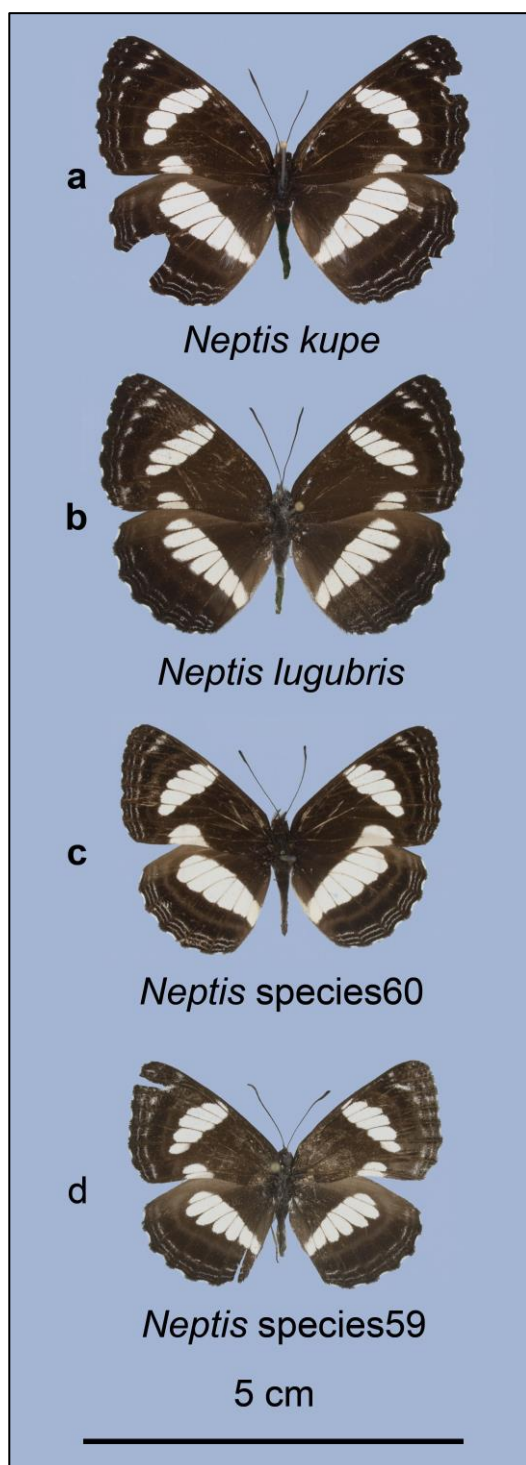


Figure 9 – Map showing capture locations for *N. kupe*, a closely related population from Tabenken, and *N. lugubris*.

Table 1 – Specimens of *Neptis kupe* examined, including specimens of a related population from Tabenken, Cameroon.

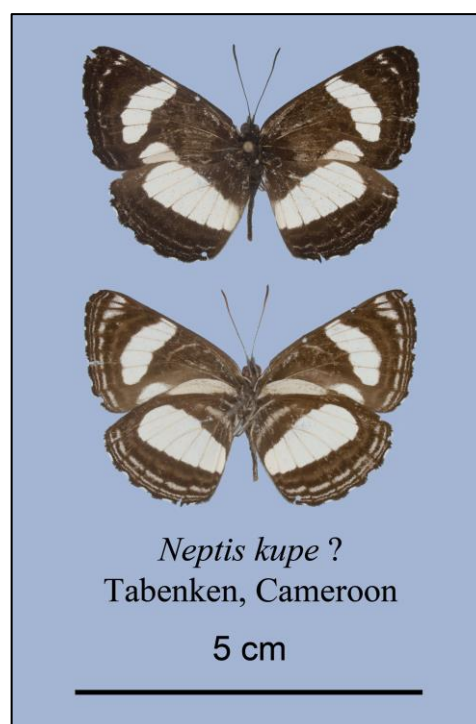
Accession number	Collection Data			Collector/s	Sex
	Locality	Elevation (m)	Date		
ABRI-152667 (barcoded)	Mt. Kupe, South West, Cameroon,	1500–1900	7–10.iv.2013	S. Sáfián, R. Tropek, M. Espeland	??
ABRI-152668 (barcoded)	Mt. Kupe, South West, Cameroon,	1500–1900	iv.2014	ABRI collector	♂
ANHRTUK 00214937	Mt. Kupe, South West, Cameroon,	1500–1900	7–10.iv.2013	S. Sáfián, R. Tropek, M. Espeland	♂
ANHRTUK 00214938	Mt. Kupe, South West, Cameroon,	1500–1900	23.i.2012	R Tropek	♀
ABRI-152914	Tabenken, North West, Cameroon	1700–2200	x–xi.2010	ABRI collector	♀
ABRI-152665	Tabenken, North West, Cameroon	1700–2200	viii.1996	S. Collins	♂
ABRI-152666	Tabenken, North West, Cameroon	1700–2200	iii.1997	S. Collins	♀

**Figure 10** – *Neptis kupe* compared with *N. lugubris* and two as yet undescribed species. **a** *N. kupe* ♂: ABRI-152668, Mt Kupe, South West, Cameroon, iv.2014; **b** *N. lugubris* ♂: ABRI-152640, Biakato, Ituri, DRC; v.2011; **c** *N. species60* ♂: Kirima, Ituri, DRC, v.2015; **d** *N. species59* ♀: Kithokolo, Nord-Kivu, DRC, iii.2012.

localities for *N. lugubris* in eastern DRC. The Tabenken specimens were too old to barcode.

Diagnosis

Neptis kupe is one of four known species with similar facies characterised by a faint or absent post-discal line on the upperside of the forewings. The submarginal lines are also weakly marked on the upperside, and the combined effect is to make the white discal bands stand out boldly. The other three species with similar facies are *N. lugubris*, *N. species59*, and *N. species60*. The latter two are not described. Single specimens of the four species are compared in Fig. 10.

**Figure 11** – Specimen collected in the Tabenken forest that could be assigned to *Neptis kupe*. ♂: ABRI-152665, Tabenken, North West, Cameroon, viii.1996; S. Collins.

In *N. kupe*, the apical section of the forewing discal band (fd3 to fd7) is crescent-shaped and convex proximad, whereas in the other three species the band is linear on the proximal edge. In all three species the hindwing discal band tapers to the inner margin; the taper is more pronounced in *N. kupe* and *N. species59* than in the other two species. A specimen from the Tabenken Forest is shown in Fig. 11 and is similar to the female of *N. kupe* illustrated in Fig. 6 cd. This is strong evidence that the Mt. Kupe and Tabenken populations are conspecific. However, it is recommended that the status of the Tabenken population remain undetermined until genetic data are available to determine the relationship between the two populations.

Etymology

Neptis kupe is named after the mountain in Cameroon, Mount Kupe (English) or Mont Koupé (French), where all known specimens have been caught. The final e in the species name should be pronounced as in the French, Koupé.

Neptis jamesi sp. nov. (Fig. 12)

urn:lsid:zoobank.org:act:E5A4EA66-C88C-44B9-B644-0C49CBCBD393

Six specimens of *N. jamesi* from the north-eastern DRC have been barcoded. One of these, a male in the ABRI collection, was selected as the holotype and is shown in Fig. 12 along with a female paratype and specimens of *N. nanciae*.

Holotype ♂: Kithokolo, Nord-Kivu, DRC, 01°10' S, 29°13' E, 1900–2000 m, xi.2014, ABRI-152959, ABRI collection.

Paratypes 2♂ and 3♀: data shown in Table 2.

Description of facies

Holotype: ♂ ABRI-152959 (Fig. 12 a, b)

Wingspan: 4.1 cm. Forewing length: 2.3 cm. Antenna-awing ratio: 0.44.

Head: Blackish; palps light brown/grey; antennae upperside dark grey/brown, antennae underside brown/grey at root grading progressively to reddish-brown at tip.

Thorax: Upperside blackish, underside marked greyish on dark brown background. Legs, pale grey distally.

Abdomen: Upperside blackish proximad grading to grey at distal extremity, underside more greyish with thin continuous light grey ventral line.

Wings: **Forewing upperside**: Convex outer margin, background colour dark brown at apex, grading to mid-brown at base and inner margin. Cell showing underside markings faintly, particularly transverse line fct2. White discal band extending from space 2A (fd1) to space R3 (fd8). Long discal band mark in space 2A (fd1) tapering to blunt point at both ends, mark in space Cu2 (fd2) broad, same length as fd1 and displaced distad relative to fd1. Proximal edges of these two marks forming line at approximately 45° to inner margin. Mark fd2 broadly separated (1.4 mm) by background colour from mark in space Cu1 (fd3). Marks in spaces Cu1 and M3 (fd3 & fd4) elongated and separated by 0.5 mm ground colour along vein Cu1, both marks elliptical and rounded at both ends. Marks in M3 and M2 (fd4 and fd5) well separated, 0.7 mm, by ground colour along the vein M3. Apical section of

discal band, marks fd5 to fd8, narrowly separated by veins and broadest in space M1 (fd6), individual marks having rounded or pointed ends distad and band deeply indented on distal edge. The final mark in space R3 (fd8) narrow coming to triangular point distad. Proximal edge of discal band marks fd6 and fd7 flat ended and fd5 strongly tapered on posterior edge. Well-defined post-discal band comprising grey marks in spaces Cu1 to R5, marks in spaces Cu1 to M2 slightly curved concave proximad. Marks in spaces M1 to R5 more or less linear. Mark in space Cu2 angled with anterior end displaced proximad. Three well defined submarginal bands of grey marks in spaces Cu2 to R5, marks in proximal band (fsm1) being linear and those in distal bands (fsm2 and fsm3) being slightly concave distad. fsm1 mark in space R5 long and curving proximad at costal end. All submarginal bands continuing into space R3 with radial mark for fsm1 and less well defined and fainter marks for fsm2 and fsm3. Postdiscal and submarginal bands appear to be greyish blue but eye-dropper tool in Photoshop shows them to be pure grey. Outer margin only slightly scalloped with patch of black cilia at end of veins and narrower patch of white cilia in between. **Forewing underside**: Background colour dark brown and noticeably lighter than upperside, spaces 2A and Cu2 much lighter. Cell markings greyish brown comprising greyish radial line along anterior edge of cell (fcr) broadening at fcr.1 and broadening again at fct1.1 at root of short and faintly marked transverse line (fct1). After short, unmarked break on anterior edge of cell, second, distal transverse line (fct2) extending across width of cell, fct2 being convex anteriad and more strongly marked than fct1. Discal band markings as on upperside. Post-discal band comprising light brown marks, broader than corresponding marks on upperside. Proximal submarginal band (fsm1) comprising broad, light brown, linear marks, well separated at veins. Further two submarginal bands (fsm2 and fsm3) clearly marked light brown, linear and narrowly separated at veins. Width of submarginal lines reducing from broadest at fsm1 to narrowest at fsm3. Two proximal submarginal bands extending from inner margin to costa. Distal band (fsm3) extending from space Cu2 to costa. Fourth submarginal band (fsm4) faintly marked in apical region from space M1 to space R3. **Hindwing upperside**: Base of wing dark brown without any markings. Spaces Rs, Sc+R1 and h lighter red brown. Discal band (hd) white, extending from inner margin (hd1) to space Rs (hd7), broadest in space M1 but not tapering significantly at inner margin. Proximal edge of band slightly concave, distal edge indented at veins and linear. Mark hd7 short and convex anteriad. Individual marks hd1 and hd2 flat ended distad grading to rounded at hd5 and hd6. Band between marks hd2 to hd6 deeply indented distad. Post-discal band faintly marked lighter than ground colour. Three submarginal bands (hsm1 to hsm3) clearly marked grey and comprising long dashes between veins, those in hsm2 and hsm3 concave distad. As on forewing, submarginal bands appear to be greyish blue but are in fact pure grey. **Hindwing underside**: broad whitish band (hb1) along costa extending from base roughly 40% of distance to apex. Two further bands, proximal band (hb2) narrow, distal band (hb3) broad and extending from inner margin curving to follow proximal band. Discal band as upperside but less sharply defined edges to individual marks. Post-discal band series of grey-brown fuzzy linear marks extending from space 2A to Sc+R1. Three grey-brown

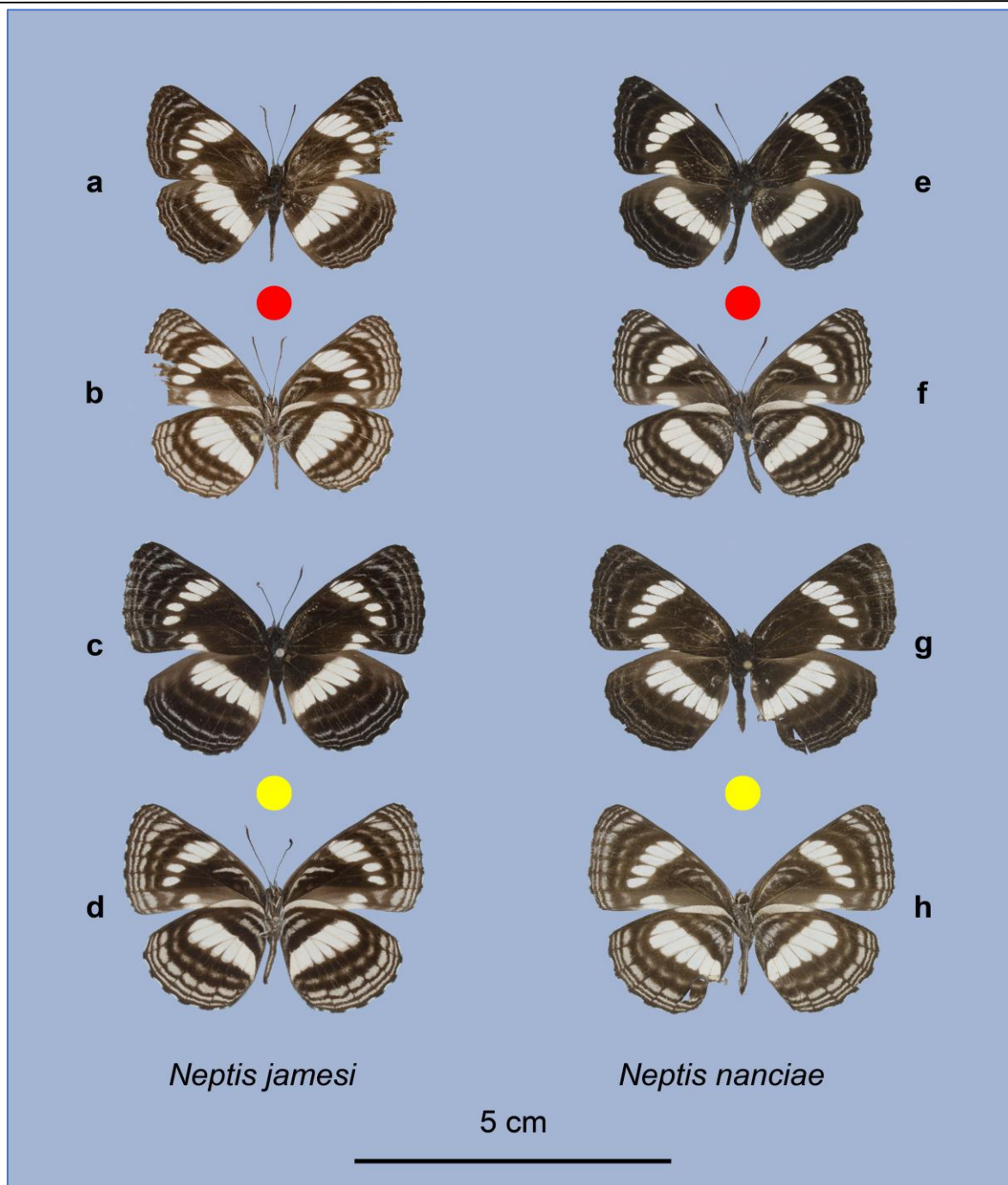


Figure 12 – *Neptis jamesi* sp. nov. and *Neptis nanciae* sp. nov. *N. jamesi* holotype ♂: ABRI-152959; Kithokolo, Nord-Kivu, DRC; xi.2014; **a** dorsal, **b** ventral. *N. jamesi* paratype ♀: IDR-A02196; Kasugho, Nord-Kivu, DRC; 15.xii.2017; R Ducarme; **c** dorsal, **d** ventral. *N. nanciae* holotype ♂: ABRI-150683; Kithokolo, Nord-Kivu, DRC; vi.2014; **e** dorsal, **f** ventral. *N. nanciae* paratype ♀: ABRI-152952; Kithokolo, Nord-Kivu, DRC; v.2012; **g** dorsal, **h** ventral.

submarginal bands well defined, proximal band (hsm1) broadest and distal bands progressively narrowing to hsm3. Proximal two submarginal bands extending from space 2A to space Rs. Distal submarginal band (hsm3) extending from Cu1 to Rs. Outer margin slightly scalloped as forewing.

Genitalia: ♂ (Fig. 13) Uncus curving uniformly ventrad with slightly hooked tip. Ventral edge of valve curved, dorsal edge also slightly curved, aspect ratio height/length = 0.26, apical process comprising straight stem terminating in flat end with ventral and dorsal hooks, ventral hook turning proximad, ventral closure narrow and coming to point, dorsal process elongated triangular shape. Aedeagus short and broad, length ratio relative to valve A/V = 0.82.

Paratype: ♀ (Fig. 12 c, d): IDR-A02196, Kasugho, Nord-Kivu, DRC, 00°15' S, 29°15' E, (-0.2500°, 29.2500°), 2000 m, vi.2014, R. Ducarme (Collection I.D. Richardson) Wingspan: 4.8 cm. Forewing length: 2.5 cm. Antenna-wing ratio: 0.43.

The description below highlights the differences between the holotype and the paratype rather than repeating elements that are almost identical.

Head: Same as holotype

Thorax: Same as holotype

Abdomen: Same as holotype except thin ventral line more clearly defined

Wings: Forewing upperside: Ground colour not significantly lighter at base and inner margin. Cell with faint underside markings like holotype. White discal band as in holotype, but marks fd2 to fd8 reduced to approximately 75% of length in holotype. Apical group of marks, fd5 to fd7, more deeply indented distad. Postdiscal and submarginal bands similar to holotype, but grey without reddish tint present in holotype (note reddish tint in the holotype may be due to specimen aging).

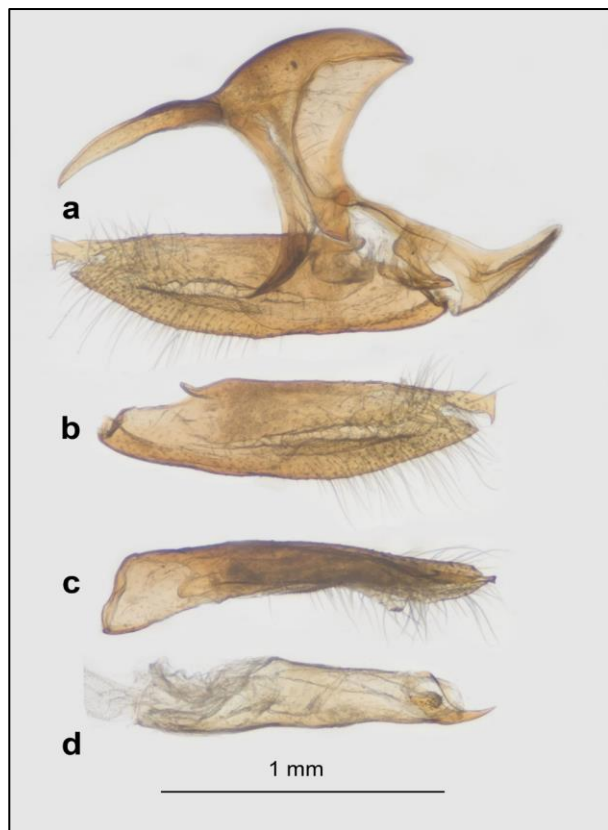


Figure 13 – Genitalia of *Neptis jamesi* ♂: **a** lateral view, **b** lateral view of valve, **c** dorsal view of valve, **d** lateral view of aedeagus ABRI-162166, Kipese, Nord-Kivu, DRC, vi.2014.

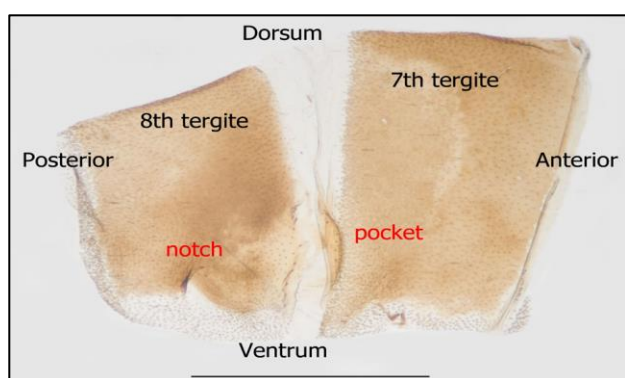


Figure 14 – *Neptis jamesi* 7th and 8th tergites of the female abdomen. Paratype ♀: IDR-A02196, Kasugho, Nord-Kivu, DRC, 15.xii.2017, R Ducarme.

Forewing underside: Similar to holotype except for reduction in lengths of discal band marks. **Hindwing upperside:** Similar to holotype with little reduction in length of discal band marks relative to holotype. Discal band tapering less towards inner margin than in holotype, both edges linear. Postdiscal and submarginal lines as in holotype male.

Genitalia: ♀ (Fig. 14) Ostium plate comprising thin clerotised border around ostium bursae, open posteriad. Well-defined pocket between 7th and 8th tergites and notch midway along ventral edge of 8th tergite.

Holotype barcode: 658 base pairs,

```
AACTTTATATTTTTATTTTTGGAATTTGAGCTGGAATA
GTAGGAACATCTCTTAGACTATTAATTGAACTGAA
TTAGGTAATCCAGGATCTTTAATTGGAGATGATCAA
ATTTATAATACTATTGTAAGTCCCATGCATTTATTA
TAATTTTTTTTATAGTTATACCTATTATAATTGGAGG
ATTTGGTAATTGATTAATTCCTAATATTAGGAGC
CCCTGACATAGCTTCCCCCGAATAAATAATATAAG
ATTCTGGCTTCTCCCCCTTCTTTAATTTTATTAATT
TCAAGTAGAATTGTAGAAACTGGAGCTGGAACAGG
ATGAACAGTATACCCTCCTTTATCTTCTAATATTGCT
CACGGCGGAGCTTCAGTAGATTTAGCTATTTTTTCC
TTACATTTAGCAGGTATTTCTTCTATTTTAGGAGCA
ATTAATTTTATTACAATATTATTAATATACGTATTA
ATAGTATATCATTTGATCAAATACCTTTACTTGTTG
ATCAGTAGGAATTACAGCTTTATTATTACTTTTATCT
TTACCTGTATTAGCTGGAGCTATTACAATATTATTA
ACAGATCGAAATTTAAATACTTTCATTTTTTGATCCT
GCTGGAGGAGGAGACCCTATTCTTTATCAACATTTA
TTT
```

Barcoding

Six specimens of *N. jamesi* yielded full length barcodes, 658 base pairs, that are allocated to BOLD BIN: ACU2951. These six barcodes have low variance with an intraspecific APD of 0.1% and a maximum PD of 0.3%, see Fig. 8. Several species have slightly smaller barcode pairwise differences with respect to *N. jamesi* than do *N. kupe* and *N. nanciae*, but these are not close relatives in the multigene phylogeny.

Material examined and distribution

Five of the barcoded specimens of *N. jamesi* were collected in medium to high elevation forest, (up to 2400 m) in Sud-Kivu province in the NE DRC and one in low elevation forest (400 m) in Sub-Ubangi province, Table 2. The presence of the species in low elevation forest suggests that its range may extend further west across much of the Congo Basin. Collection localities for the six specimens are plotted on the map, Fig. 15, along with collection localities for *N. nanciae*.

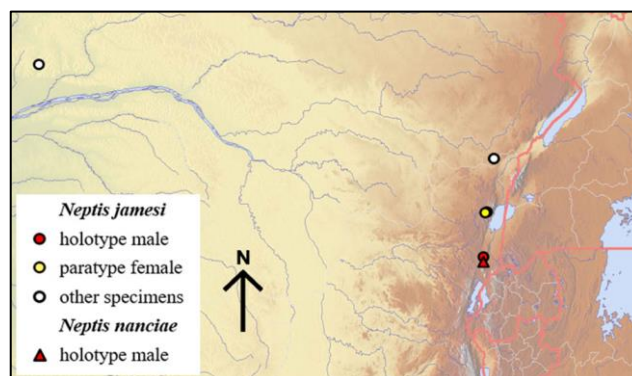


Figure 15 – Map showing the capture localities for barcoded specimens of *Neptis jamesi* and *Neptis nanciae*. Note that the holotypes of *N. jamesi* and *N. nanciae* were captured at the same locality and the markers have been displaced N and S of the true locality so that both markers are visible.

Table 2 – Specimens of *Neptis jamesi* examined.

Accession number	Collection Data			Collector/s	Sex
	Locality	Elevation (m)	Date		
ABRI-152947	Mamove, Nord-Kivu, DRC	1000	ii.2011	ABRI collector	♀
ABRI-152948	Mamove, Nord-Kivu, DRC	1000	ii.2011	ABRI collector	♀
ABRI-152959 Holotype ♂	Kithokolo, Nord-Kivu, DRC	1900–2000	xi.2014	ABRI collector	♂
ABRI-162166	Kipese, Nord-Kivu, DRC	2400	vi.2014	ABRI collector	♂
ABRI-163589	Kwokoro, Sud-Ubangi, DRC	400	iv-vi 2016	ABRI collector	♂
IDR-A02196 Paratype ♀	Kasugho, Nord-Kivu, DRC	2000	15.xii.2017	R. Ducarme	♀

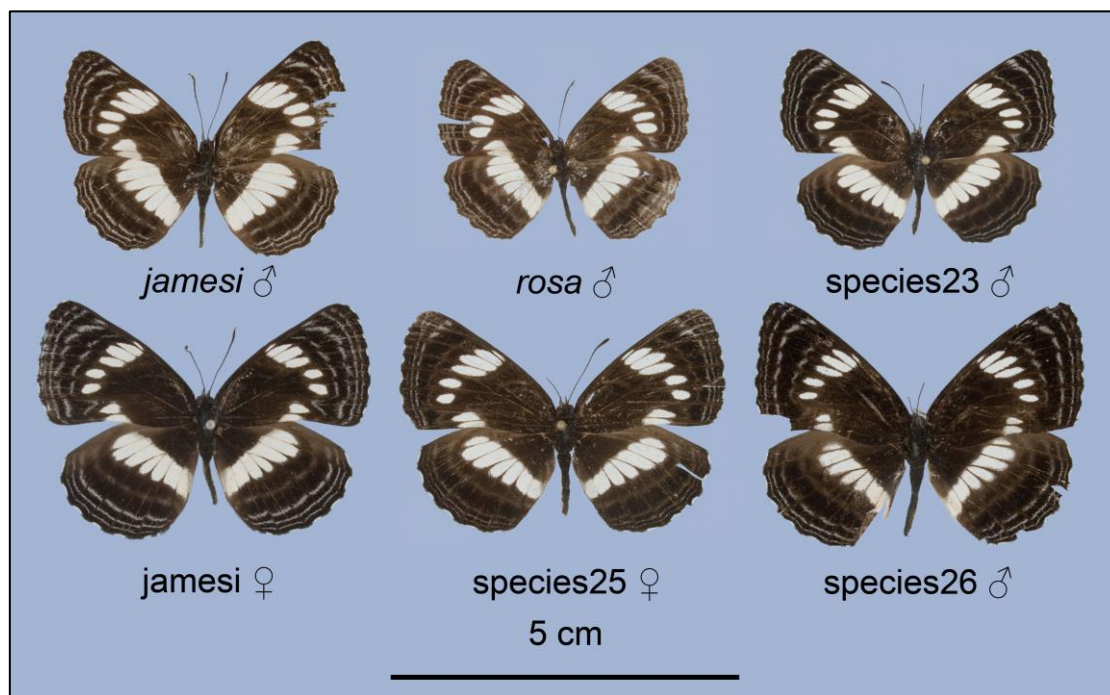


Figure 16 – *Neptis jamesi* compared with specimens of four other *Neptis* species. *N. jamesi* holotype ♂: ABRI-152959, Kithokolo, Nord-Kivu, DRC, xi.2014; *N. rosa* Pierre-Baltus & Pierre, 2007 ♂: ABRI-153087, Makele, Ituri, DRC, xii.2014; *N. species23* ♂: ABRI-152925, Mamove, Nord-Kivu, DRC, iii.2012; *N. jamesi* paratype ♀: IDR-A02196, Kasugho, Nord-Kivu, DRC, 15.xii.2017, R Ducarme; *N. species25* ♀: ABRI-152926, Kithokolo, Nord-Kivu, DRC, v.2012; *N. species26* ♂: ABRI-152930, Manzumbu, Ituri, DRC, ix.2014.

Diagnosis

The forewing discal bands in *N. jamesi* have a distinctive wing pattern, two marks at the inner margin (fd1 and fd2), two well separated oblong marks (fd3 and fd4) and a more contiguous block of three marks (fd5 to fd7) near the costa. However, two factors nullify this distinctive pattern as a diagnostic character:

1. There are several other species, not closely related to *N. jamesi*, that have a similar pattern.
2. *N. jamesi* is variable in terms of the size and separation of the forewing discal bands marks as can be seen in the two specimens illustrated in Fig. 16. The male has radially long marks whereas in the female the marks are much shorter.

Six specimens are illustrated in Fig. 16, including the holotype and paratype female of *N. jamesi*, showing variations of a common wing pattern. Although criteria can be proposed to separate the individual specimens, these break down for the wider populations of each species owing to intra-species variability. The only species of those illustrated that can be separated reliably on the facies is *N. species26*, which consistently has a more falcate

forewing than the other four species. No such criteria have been identified to separate the other four species.

Neptis jamesi can, however, be separated unambiguously from these four species, and others with similar facies, by its barcode sequence. The interspecific barcode average pairwise difference (APD) values with respect to *N. jamesi* are as follows:

- *N. rosa* Pierre-Baltus C. & Pierre J., 2007, APD = 6.6%
- *N. species23* APD = 7.6%
- *N. species25* APD = 6.5%
- *N. species26* APD = 6.2%

Etymology

The third author has named the taxon *Neptis jamesi* in honour of his son James.

Neptis nanciae sp. nov. (Fig. 12)

urn:lsid:zoobank.org:act:827BCF93-A0F2-4FCA-A2B2-6C7E682BC119

Two specimens of *N. nanciae* from high elevation forest in the north-eastern DRC have been barcoded. One of these, a male in the ABRI collection, is selected as the holotype and is shown in Fig. 12 along with a female paratype and specimens of *Neptis jamesi*.

Holotype: ♂ Kithokolo, Nord-Kivu, DRC, 01°10' S, 29°13' E, (-1.1667°, 29.2167°), 1900–2000 m, vi.2014, ABRI-150683, ABRI collection.

Paratype: ♀ Kithokolo, Nord-Kivu, DRC, 01°10' S, 29°13' E, (-1.1667°, 29.2167°), 1900–2000 m, v.2012, ABRI-152952, ABRI collection

Description of facies

Holotype: ♂ ABRI-150683 (Fig. 12 e, f)

Wingspan: 4.1 cm. Forewing length: 2.4 cm. Antenna-wing ratio: 0.46.

Head: Blackish; palps light brown/grey; antennae upperside dark grey/brown, antennae underside brown/grey at root grading progressively to dark reddish-brown at tip.

Thorax: Upperside blackish, underside dark brown. Legs, grey distally.

Abdomen: Upperside blackish, underside more greyish with thin continuous light grey ventral line and thin light grey lateral lines.

Wings: Forewing upperside: Background colour dark brown to black at apex, grading to a slightly lighter shade at base and inner margin. Cell unmarked. Discal band composed of white marks extending from space 2A at inner margin to space R3 at costa. Elongated discal band mark in space 2A (fd1) tapering to blunt point distad and with flat angled proximal end, mark in space Cu2 (fd2) broad, slightly shorter than fd1. The proximal edges of these two marks forming line at approximately 60° to inner margin. Mark fd2 broadly separated (2.0 mm) by background colour from mark in space Cu1 (fd3). Mark fd3 short, rounded proximad and almost flat distad, angled with distal end displaced posteriad. fd3 only narrowly separated from fd4, Broad mark rounded at both ends and narrowly separated from fd5 by ground colour. Apical marks fd5 to fd7 longer and almost contiguous only narrowly separated by veins, fd6 longest. fd8 long thin linear mark in space R3. Band from fd3 to fd7 deeply indented at veins on distal edge. Proximal edge of discal band marks fd4 to fd7 flat ended and fd5 strongly tapered on posterior edge. Proximal edge of discal band making angle of approximately 25° between fd3 to fd4 and fd5 to fd7. Faintly marked post-discal band comprising indistinct brownish marks in spaces Cu2 to R5. Two submarginal bands of grey linear marks in spaces Cu2 to R3. fsm1 mark in space R5 long and angled proximad at costal end. Both submarginal bands continuing into space R3 with well-defined mark for fsm1 and less well defined and fainter mark for fsm2. fsm2 generally more weakly marked than fsm1 and individual marks broadly separated in apical area. Submarginal bands appear to be greyish blue but are in fact pure grey. Outer margin scalloped with broad patch of black cilia at end of veins and narrow patch of white cilia in between.

Forewing underside: Background colour dark brown and lighter than upperside, the spaces 2A and Cu2 much lighter. Cell markings greyish brown comprising narrow greyish radial line along anterior edge of cell (fcr) broadening at fcr.1 and broadening again at fct1.1 at root of short and faintly marked transverse line (fct1). After short, unmarked break on anterior edge of cell, second, distal transverse line (fct2) extending across width of cell, fct2 being convex anteriad and more strongly marked than fct1. Discal band markings creamy white as on upperside,

but less sharply defined at edges. Post-discal band comprising greyish-brown marks, broader than on upperside, marks in spaces M3 to M1 concave proximad, other marks linear, mark in Cu2 displaced proximad. Proximal submarginal band (fsm1) comprising broad, light brown, linear marks, broadly separated at veins. Further two submarginal bands (fsm2 and fsm3) clearly marked light brown, linear and more narrowly separated at veins. Width of submarginal lines reducing from broadest at fsm1 to narrowest at fsm3. Two proximal submarginal bands extending from inner margin to costa. Distal band (fsm3) extending from space Cu2 to costa. **Hindwing upperside:** Base of wing ground coloured without any markings. Spaces Rs, Sc+R1 and h lighter red brown. Discal band (hd) white, extending from inner margin (hd1) to space Rs (hd7), broadest in space M1 (hd6), tapering to inner margin where mark hd1 is roughly half length of hd6. Band curves slightly proximad at inner margin. Mark hd7 short and convex anteriad. Individual marks hd1 to hd6 flat ended distad or rounded. Post-discal band faintly marked lighter than ground colour. Three submarginal bands (hsm1 to hsm3) clearly marked grey and comprising long linear dashes between veins. As on forewing, submarginal bands appear to be greyish blue but are in fact pure grey. Outer margin scalloped with tufts of black scales at end of veins and white cilia in between. **Hindwing underside:** Broad whitish band (hb1) along costa extending from base

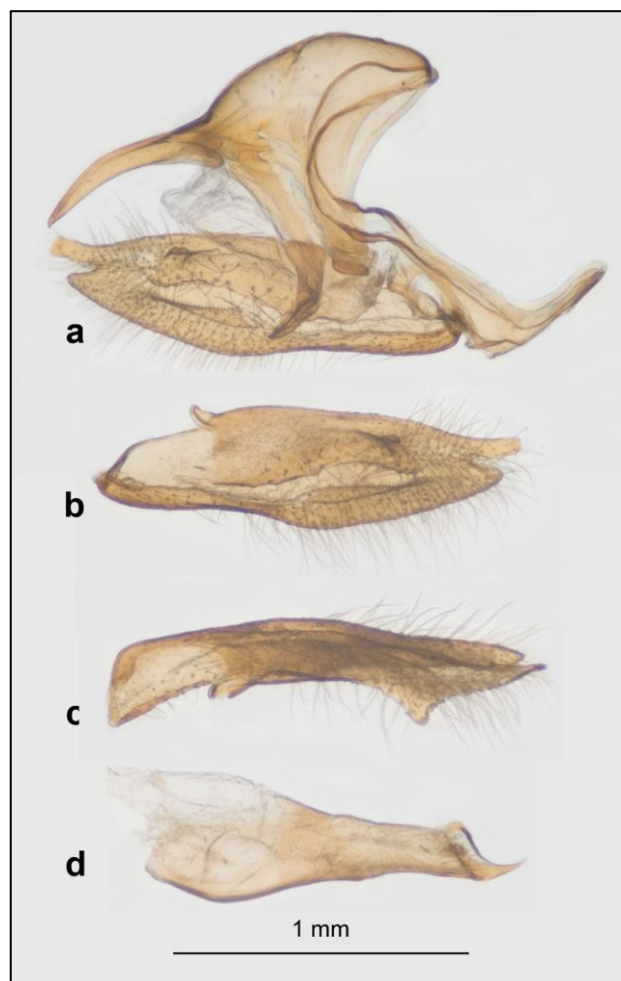


Figure 17 – Genitalia of *Neptis nanciae* holotype ♂: **a** lateral view of genitalia, **b** lateral view of valve, **c** dorsal view of valve, **d** lateral view of aedeagus. ABRI-150683, Kithokolo, Nord-Kivu, DRC; vi.2014, ABRI collection.

roughly 45% of distance to apex. Two further bands, proximal band (hb2) narrow, distal band (hb3) broad and extending from inner margin curving to follow proximal band. Discal band as upperside but less sharply defined edges to individual marks. Post-discal band series of grey-brown linear marks extending from space 2A to Sc+R1. Three grey-brown submarginal bands well defined, proximal band (hsm1) broadest and distal bands progressively narrowing to hsm3. Proximal two submarginal bands extending from space 2A to space Rs. Distal submarginal band (hsm3) extending from Cu2 to Rs.

Genitalia: ♂ (Fig. 17) Uncus curving uniformly ventrad with hooked tip. Ventral edge of valve curving from ventral closure to mid-point, the broadest point of valve, then curving convex. Dorsal edge curving from base of apical process about $\frac{2}{3}$ of length of valve. Stem of apical process angled dorsad relative to dorsal edge of valve. Form of terminal structure of apical process unknown as this has been broken off both valves. Aspect ratio height/length = 0.27. Dorsal process elongated triangular shape. Aedeagus short and broad, length ratio relative to valve, A/V = 0.90.

Paratype: ♀ (Fig. 12 g, h): Kithokolo, Nord-Kivu, DRC, 01°10' S, 29°13' E, (-1.1667°, 29.2167°), 1900–2000 m; v.2012, ABRI-152952, ABRI collection.

Wingspan: 4.9 cm. Forewing length: 2.7 cm. Antenna-wing ratio: unknown.

Description below highlights differences between holotype and paratype rather than repeating elements that are almost identical.

Head: Same as holotype

Thorax: Same as holotype

Abdomen: Same as holotype except lateral line broader

Wings: Forewing upperside: Background colour more reddish than in holotype, possibly due to age of specimen. Discal band as holotype except that 25° angle formed by proximal edge is less apparent due to projection of fd4 proximad. Third submarginal band, fsm3, faintly visible from space M3 to apex. **Forewing underside:** Proximal transverse line fct1 in cell clearly marked whilst it is faint in holotype male. **Hindwing upperside:** Vein Rs coloured with light brown scales, not present in holotype.

Hindwing underside: Same as holotype.

Genitalia: ♀ (Fig. 18)

Ostium plate comprising thin sclerotised border around ostium bursae, open posteriad. Well-defined pocket between 7th and 8th tergites and weakly defined notch midway along ventral edge of 8th tergite.

Distance between notch and pocket is consistent with distance between dorsal process and apical process of valve, bearing in mind that tip of apical process is missing.

Holotype barcode: 658 base pairs,

AACTTTATATTTTATTTTTGGAATCTGAGCTGGAA
TAGTCGGTACATCTCTTAGTTTACTAATCCGAACT
GAATTAGGTAATCCAGGATCTTTAATTGGAGATG
ATCAAATTTATAATACTATTGTAAGTCCCATGC
ATTTATTATAATTTTTTTTATAGTTATACCTATTA
TAATTGGAGGATTTGGTAATTGATTAATTCCTTTA
ATATTAGGAGCTCCTGATATAGCTTTCCCCCGAA
TAAATAACATAAGATTTTGACTTCTCCCTCCTTCT

TTAATTTTACTAATTTCTAGTAGAATTGTAGAAA
CTGGAGCTGGAACAGGATGAACAGTATACCCCC
CTCTATCTTCTAATATTGCCCATAGTGGAGCTTCT
GTAGATTTAGCAATTTTTTCTTTACATTTAGCAGG
TATTTCTTCTATTTTAGGAGCAATTAATTTTATTA
CAACTATTATTAATATACGCATTAATAATATATC
ATTTGATCAAATACCTTTATTTGTTTGATCAGTAG
GAATTACAGCTTTACTATTACTTTTATCTTTACCT
GTATTGGCCGGAGCTATTACAATATTACTAACAG
ATCGAAATTTAAATACTTTCATTTTTTTGATCCTGCT
GGAGGAGGAGATCCTATTCTTTATCAACATTTAT
TT

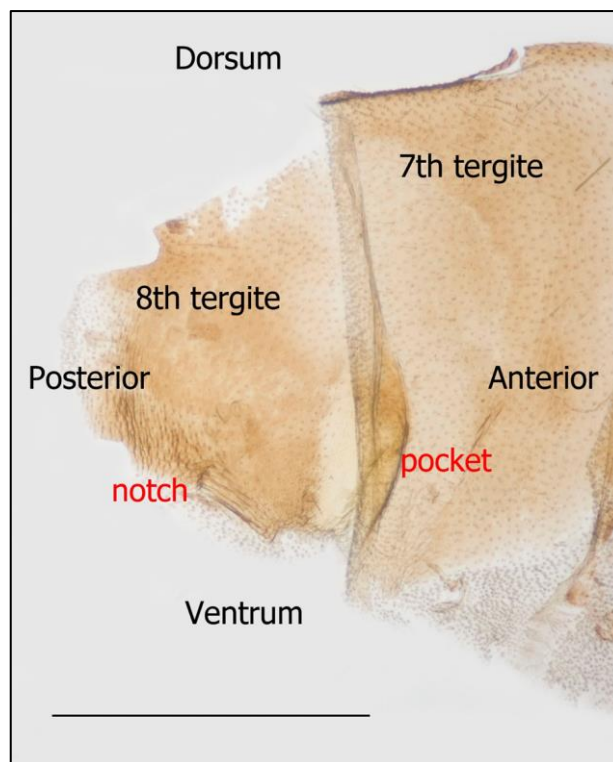


Figure 18 – *Neptis nanciae* 7th and 8th tergites of the female abdomen. Paratype ♀: Kithokolo, Nord-Kivu, DRC, v.2012, ABRI-152952, ABRI collection.

Barcoding

The two specimens of *N. nanciae* yielded identical full-length barcodes, 658 base pairs, that are included in BOLD BIN ACU3559. The APD between *N. nanciae* and specimens of *N. kupe* and *N. jamesi* ranges from 5.2% to 5.6%, see Fig. 8. Although other species have a lower APD with respect to *N. nanciae*, the multi-gene phylogeny does not show these species as close relatives.

Material examined and distribution

Both barcoded specimens of *N. nanciae* were collected in high elevation forest at Kithokolo in Sud-Kivu province in the NE DRC, but not on the same occasion. The collection localities for the two specimens are plotted on the map, Fig. 15, and detailed in Table 3.

Diagnosis

Specimens of three species are shown in Fig. 19 that might be easily confused with *N. nanciae*, the holotype male and paratype female are shown in the left-hand column.

Table 3 – Specimens of *N. nanciae* examined

Accession number	Capture Data			Collector/s	Sex
	Locality	Elevation (m)	Date		
ABRI-150683 Holotype ♂	Kithokolo, Nord-Kivu, DRC	1900–2000	xi.2014	ABRI collector	♂
ABRI-152952 Paratype ♀	Kithokolo, Nord-Kivu, DRC	1900–2000	v.2012	ABRI collector	♀

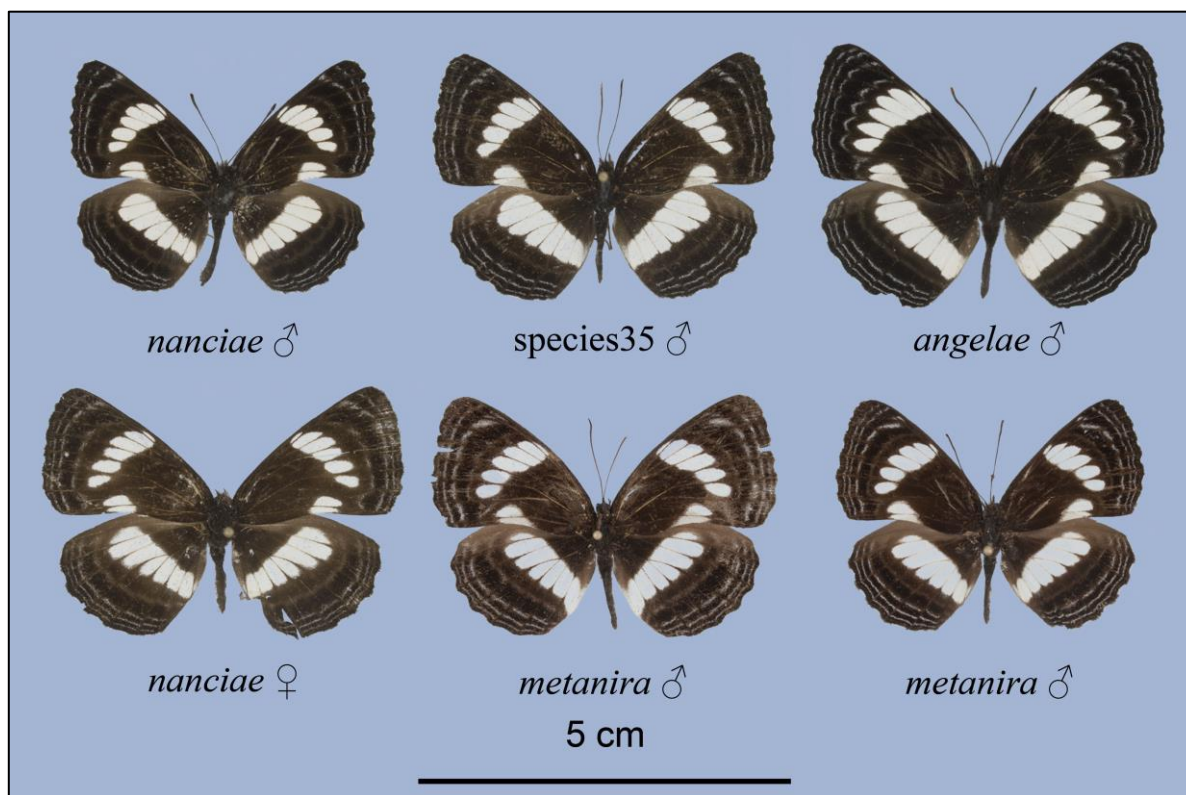


Figure 19 – *Neptis nanciae* compared with specimens of three other species: *N. nanciae* holotype ♂: ABRI-150683, Kithokolo, Nord-Kivu, DRC; vi.2014; *N. species35* ♂: ABRI-152965, Kanyasi, Ituri, DRC; i.2015; *N. angelae* sp. nov. ♂: ABRI-150658; Ekombe, Equateur, DRC; vii.2014; *N. nanciae* paratype ♀: ABRI-152952, Kithokolo, Nord-Kivu, DRC; v.2012; *N. metanira* ♂: ABRI-162155, Lubango, Nord-Kivu, DRC; vi.2016; *N. metanira* ♂: ABRI-152969, Mamove, Nord-Kivu, DRC; ii.2014.

The facies of the two specimens of *N. nanciae* differ in the form of the forewing discal band, which broadens towards the costa in the male, fd6 & fd7, and is of almost constant width in the female. This is indicative of variability within the species, and this will tend to make identification more difficult. Taking each of the three species in turn, diagnostic characters are proposed where possible.

Neptis angelae sp. nov., is easily separated on the form of the marks making up the postdiscal line, fpd, and inner submarginal line, fsm1, on the forewing. In *N. angelae*, these marks are crescent shaped, concave proximally, whereas in *N. nanciae* they are linear. The distinction is clearest on the forewing underside.

In *N. metanira* the hindwing discal band, hd, curves slightly distad at the inner margin (confirmed in 8 barcoded specimens). By contrast, in *N. nanciae* the hindwing discal band curves slightly proximad at the inner margin. This is, however, a rather weak diagnostic character.

The undescribed *N. species35* is more problematic as no diagnostic character can be seen to separate it from *N. nanciae*. It can be seen in Fig. 19 that the hindwing discal band is broader in *N. species35*. However, this is a variable character in many species within the Nysiades

group and cannot be relied upon to differentiate these two species.

N. nanciae can, however, be separated unambiguously from all three species, and others with similar facies, by the barcode. The barcode interspecific APD values with respect to *N. nanciae* are:

- *N. angelae* APD = 7.3%
- *N. species35* APD = 6.9%
- *N. metanira* APD = 5.9%

Etymology

The third author has named the taxon *N. nanciae* in honour of his daughter Nancy.

Lugubris subgroup

Neptis angelae sp. nov. (Fig. 20)

urn:lsid:zoobank.org:act:D43C9ECB-96D1-4B12-8A37-0D0B843BD2E7

Only one male specimen of *N. angelae* is known to date, from Ekombe, Équateur province in the DRC. The specimen was captured during an ABRI sponsored expedition to revisit localities recorded by reverend father Gustaaf Hulstaert (1900–1990), a Belgian missionary

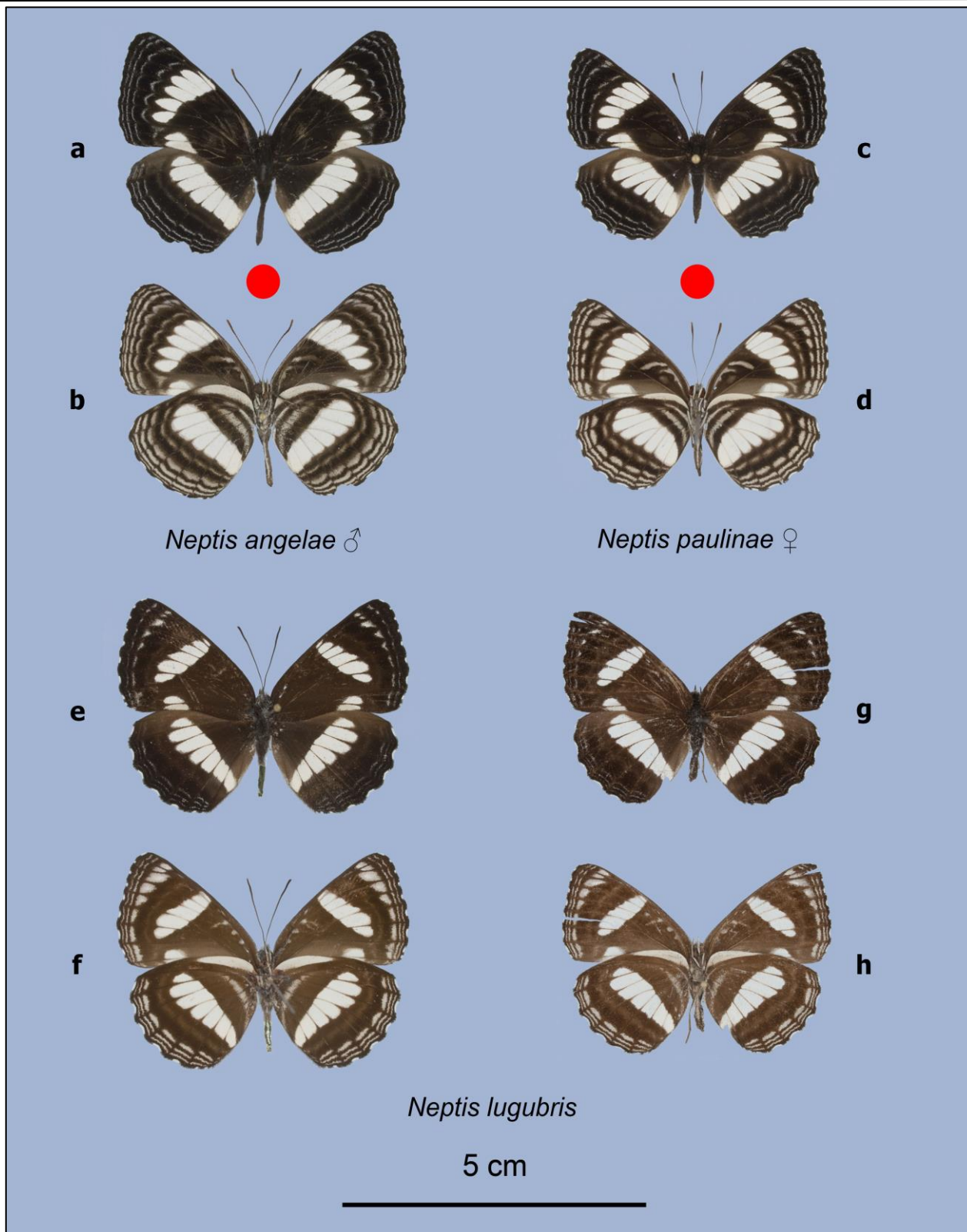


Figure 20 – *Neptis angelae* sp. nov., *Neptis paulinae* sp. nov., and *Neptis lugubris* Rebel, 1914: *N. angelae* holotype ♂: ABRI-150658, Ekombe, DRC, ix.2014, **a** dorsal, **b** ventral; *N. paulinae* holotype ♀: ABRI-162726, Otto Maber, DRC, ix.2016, **c** dorsal, **d** ventral; *N. lugubris* ♂: ABRI-152640, Biakato, DRC, vi 2011, **e** dorsal, **f** ventral; *N. lugubris* ♀: ABRI-152648, Kibale, DRC, vi 2013, **g** dorsal, **h** ventral.

belonging to the Missionnaires du Sacré-Cœur de Jésus. The single specimen is in the ABRI collection and is selected as the holotype, see Fig. 20 along with specimens of the other two related species.

Holotype: ♂ Ekombe, 73km Mbandaka, Équateur province, DRC, 00°24' S, 18°23' E, (-0.4000°, 18.3833°),

330 m, ix.2016, ABRI-150658, ABRI collection.

Paratypes: None

Description of facies

Holotype: ♂ ABRI-152952 (Fig. 20 a, b)
Wingspan: 4.8 cm. Forewing length: 2.8 cm. Antenna-
wing ratio: 0.41.

Head: Black; palps greyish brown; antennae upperside dark grey/brown at the root, darkening progressively distad with indistinct dark brown patch at tip, antennae underside mid grey at root grading progressively to darker grey towards tip and then dark brown at tip.

Thorax: Upperside black, underside marked greyish on dark brown background. Legs, whitish distally.

Abdomen: upperside almost black, no markings along sides, thin continuous grey ventral line.

Wings: Forewing upperside: Background colour black. Cell unmarked. Discal band extending from space 2A (fd1) to space R3 (fd8). Long discal band mark in space 2A (fd1) tapering both proximad and distad, mark in space Cu2 (fd2) shorter than fd1 and tapering in same way, broadly separated (2 mm) by background colour from mark in space Cu1 (fd3). Marks in spaces Cu1 and M3 (fd3 & fd4) separated narrowly by ground colour along vein Cu1, both marks tapering to point distad and flat ended proximad. Marks in M3 and M2 (fd4 and fd5) narrowly separated by ground colour along vein M3. Discal band broadening progressively in spaces M2 to R5 (fd5 to fd7) with rounded ends distad and band deeply indented on distal edge. Final mark in space R3 (fd8) narrow triangular shape pointed distad. Proximal edge of discal band marks flat ended and forming roughly 30° angle at vein M3. Well-defined post-discal band comprising grey crescent shaped marks, concave proximad, in spaces Cu2 to R5, mark in Cu2 being displaced proximad. Three well defined submarginal bands of grey marks in spaces Cu2 to R3, marks in proximal band (fsm1) being curved, concave proximad, and those in distal two bands (fsm2 and fsm3) being linear. The postdiscal and submarginal bands appear to be greyish blue but eyedropper tool in Adobe Photoshop shows them to be pure grey. Outer margin only slightly scalloped with broad patch of black cilia at end of veins and white cilia in between. **Forewing underside:** Background colour dark brown and noticeably lighter than upperside. Cell markings greyish brown comprising radial line along anterior edge of cell (fcr) marked with well-defined spot (fcr.1) and terminating in spot (fct1.1) at root of faint transverse line (fct1). After short, unmarked break on anterior edge of cell, another larger, spot (fct2.1) at root of second, distal transverse line (fct2). Discal band markings as on upperside, but less sharply defined at edges. Post-discal band more distinctly marked, greyish-brown, than on upperside. Proximal submarginal band (fsm1) comprising curved marks, concave proximally, narrowly separated at veins. Further three submarginal bands (fsm2 to fsm4) clearly marked greyish-brown and only narrowly separated at veins. fsm2 broadest of the three with individual marks slightly concave proximad, fsm3 and fsm4 progressively narrower with linear marks. Three proximal submarginal bands extending from inner margin to costa. Distal band (fsm4) extending from costa into space Cu2 where it is faint. **Hindwing upperside:** Base of wing ground coloured without any markings. Discal band (hd) extending from inner margin (hd1) to space Rs (hd7), broadest in space M2 but not tapering significantly at inner margin. Band is slightly indented at veins distad. The mark hd7 short and convex anteriorly. Individual marks flat ended distad. Post-discal band faintly marked lighter than ground colour. Three submarginal bands (hsm1 to hsm3) clearly marked grey and comprising long dashes between veins. As on

forewing, submarginal bands pure grey. **Hindwing underside:** Broad whitish band (hb1) along costa extending from base roughly halfway to apex. Two further bands, proximal band (hb2) narrow and extending from inner margin and curving to almost parallel with costa, distal band (hb3) broad and extending from inner margin curving to follow proximal band. Discal band as upperside but less sharply defined edges to individual marks. Post-discal band series of grey-brown linear marks extending from space 2A to Sc+R1. Four grey-brown submarginal bands well defined, proximal band (hsm1) broadest and distal bands progressively narrowing to hsm4. Proximal three submarginal bands extending from space 2A to space Rs. The distal submarginal band (hsm4) extending from Cu1 to M1. Outer margin slightly scalloped as forewing.

Genitalia: ♂ (Fig. 21) Uncus curving uniformly ventrad with hooked tip, valve broad in vertical plane at about mid-point and tapering from pronounced peak at about 1/3 of way along ventral edge. Apical process comprising stem terminating with robust hook curving ventrad and proximad. Aedeagus/valve length ratio 1.06, aedeagus having short slightly curved spine. Note that in Fig. 21a, hooked tip of apical process of valve is missing.

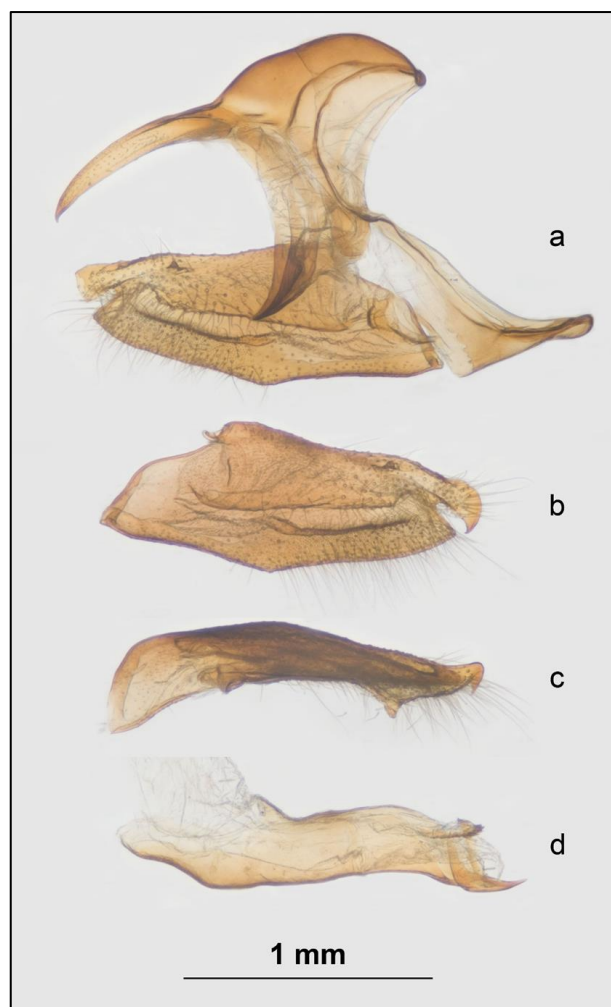


Figure 21 – Male genitalia of *N. angelae* sp. nov. ABRI-150658, Ekombe, DRC, ix.2016. **a** Genitalia with aedeagus and right valve removed, **b** right valve lateral view, **c** right valve dorsal view **d** aedeagus lateral view. **Note:** the tip of the apical process of the valve in image **a** is missing.

Holotype barcode: 658 base pairs.

AACTTTATATTTTATCTTTGGAAATTTGGGCTGGAAT
AGTAGGTACATCTCTTAGTTTATTAATTCGAACTGA
ATTAGGTAATCCAGGATCTTTAATCGGAGATGATCA
AATTTATAATACTATTGTAACCTGCTCATGCATTTATC
ATAATTTTTTTTTATAGTTATACCTATTATAATTGGAG
GATTTGGTAATTGACTAATTCCTTTAATATTAGGAG
CTCCTGACATAGCTTTCCCCCGAATAAATAATATAA
GATTTGACTTCTCCCCCTCTTTAATTTTATTAAT
TTCTAGTAGAATTGTAGAACTGGAGCTGGAACAG
GATGAACAGTTTACCCCCCTATCTTCAAATATCG
CTCACGGTGGAGCTTCTGTAGATTTAGCTATTTTTTC
ATTACATCTAGCAGGTATTTCTATTTTTAGGGGC
AATTAATTTTATTACAACATTTATTAATATACGCATT
AATAGAATGGCATTTCGATCAGATACCTTTATTTGTT
TGATCGGTAGGAATTACAGCCTTATTACTCCTA
TCTTTACCTGTATTAGCTGGAGCTATTACAATACTA
TTAACAGACCGAACTTAAATACTTCATTTTTTGAT
CCTGCTGGAGGGGGAGATCCTATTCTTTATCAACAT
TTATTT

Barcoding

The single specimen of *N. angelae* yielded a full-length barcode, 658 base pairs, that is allocated to BOLD BIN ACU3565. Although several species have smaller barcode pairwise differences with respect to *N. angelae* than do *N. lugubris* and *N. paulinae*, these are not recovered as close relatives in the multi-gene phylogeny. The barcodes do, however, demonstrate that the three species *N. lugubris*, *N. angelae* and *N. paulinae* are well separated from each other as can be seen in the Klee diagram, Fig. 22.

	Country	DRC	DRC	Gabon	DRC	DRC	DRC
Country	Species	<i>paulinae</i>	<i>angelae</i>	<i>lugubris</i>	<i>lugubris</i>	<i>lugubris</i>	<i>lugubris</i>
DRC	<i>paulinae</i>						
DRC	<i>angelae</i>	7.5					
Gabon	<i>lugubris</i>	6.5	6.6				
DRC	<i>lugubris</i>	6.8	6.6	0.6			
DRC	<i>lugubris</i>	6.8	6.6	0.6	0.0		
DRC	<i>lugubris</i>	6.8	6.6	0.6	0.0	0.0	

Figure 22 – Klee diagram with barcode pairwise differences within species subgroup *N. lugubris*, *N. angelae* and *N. paulinae*.

Material examined and distribution

The species *N. angelae* is known from a single male captured near Ekombe in Équateur province in the NW DRC. This specimen, the holotype, is in the ABRI collection in Nairobi. The collection locality for the specimen is plotted on the map, Fig. 23, along with collection localities for *N. paulinae* and barcoded specimens of *N. lugubris* in the ABRI collection.

Diagnosis

Neptis angelae can be separated from other *Neptis* species by the form of the post-discal and first submarginal bands on the underside of the forewing. These bands comprise crescent shaped marks strongly **convex distad**. Some other

Neptis species have one or both of these bands (fpd and fsm1) comprising crescent shaped marks, but **convex proximad**. Additional diagnostic characters for this species are the pronounced broadening of the forewing discal band towards the costa (fd5 to fd7) and the deep indentation of the forewing discal band from fd3 to fd7 on the distal edge.

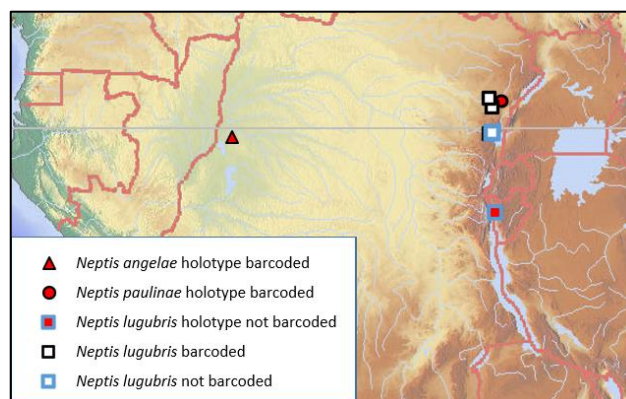


Figure 23 – Map showing capture localities for *N. angelae*, *N. paulinae* and *N. lugubris*

Neptis paulinae sp. nov. (Fig. 20)

urn:lsid:zoobank.org:act:8D253114-0AC5-4325-B114-64421E0C5B3B

Only one female specimen of *N. paulinae* is known from Otto Maber, Ituri province in the DRC. The specimen is in the ABRI collection and is selected as the holotype. The specimen is shown in Fig. 20 along with specimens of the other two related species.

Holotype ♀: Otto Maber, Ituri province, DRC, 01°04'32" N, 29°35'17" E, (1.0756°, 29.5881°), 1050 m, ix.2016, ABRI-162726, ABRI collection.

Paratypes: None

Description of facies

Holotype: ABRI-162726 (Fig. 20 c, d)

Wingspan: 4.3 cm. Forewing length: 2.5 cm. Antenna-wing ratio: 0.43.

Head: Black; palps light grey; antennae upperside dark grey/brown with indistinct more reddish-brown patch at tip, antennae underside mid grey at root grading progressively to darker grey towards tip and then dark reddish brown at tip.

Thorax: Upperside almost black, underside marked greyish on dark brown background. Legs, whitish distally.

Abdomen: Upperside almost black, underside more greyish with thin continuous light grey ventral line, thin continuous light grey line along sides.

Wings: Forewing upperside: Background colour dark brown to black. Cell showing underside markings faintly. Long discal band mark in space 2A (fd1) tapering to narrow point distad and less sharply proximad, mark in space Cu2 (fd2) shorter than fd1 and tapering in same way but more rounded distad. The proximal edges of these two marks form line at approximately 45deg to inner margin. The mark fd2 broadly separated (1.5 mm) by background colour from mark in space Cu1 (fd3). Marks in spaces Cu1 and M3 (fd3 & fd4) separated narrowly by ground colour along vein Cu1, both marks rounded distad and flat ended proximad. Marks in M3 and M2 (fd4 and fd5) narrowly

separated by ground colour along vein M3. Discal band broadest in space M1 (fd6) individual marks having rounded ends distad and band deeply indented on distal edge. Final mark in space R3 (fd8) narrow triangular shape pointed distad. Proximal edge of discal band marks flat ended and forming roughly 30° angle at vein M3. Well-defined post-discal band comprising grey marks in spaces Cu2 to R5, marks in spaces Cu1 to R5 slightly curved and colinear. Mark in space Cu2 displaced proximad and angled with anterior end displaced proximad. Three well defined submarginal bands of grey marks in spaces Cu2 to R3, marks in proximal bands (fsm1 and fsm2) being linear and those in distal bands (fsm3) being slightly concave distad. Postdiscal and submarginal bands appear to be greyish blue but eye-dropper tool in Photoshop shows them to be pure grey. Outer margin only slightly scalloped with broad patch of black cilia at end of veins and narrower patch of white cilia in between. **Forewing underside:** Background colour dark brown and noticeably lighter than upperside, spaces 2A and Cu2 much lighter. Cell markings greyish brown comprising radial line along anterior edge of cell (fcr) broadening at fcr.1 and broadening again at fct1.1 at root of short transverse line (fct1). After short, unmarked break on anterior edge of cell, second, distal transverse line (fct2) extending across width of cell, fct2 being convex anteriad. Discal band markings as on upperside, but less sharply defined at edges. Post-discal band comprising greyish-brown marks, broader than on upperside, marks in spaces 2A and Cu2 forming semicircle around distal ends of fd1 and fd2. Proximal submarginal band (fsm1) comprising broad, light brown, linear marks, broadly separated at veins. Further two submarginal bands (fsm2 and fsm3) clearly marked light brown, linear and only narrowly separated at veins. Width of submarginal lines reducing from broadest at fsm1 to narrowest at fsm3. Two proximal submarginal bands extending from inner margin to costa. The distal band (fsm3) extending from space Cu2 to costa. **Hindwing upperside:** Base of wing ground coloured without any markings. Spaces Rs, Sc+R1 and h lighter reddish brown. Discal band (hd) extending from inner margin (hd1) to space Rs (hd7), broadest in space M1 (hd6) but not tapering significantly at inner margin. Distal edge of band indented at veins. Mark hd7 short and convex anteriad. Individual marks hd1 and hd2 flat ended distad grading to rounded at hd5 and hd6. Band between marks hd2 to hd6 deeply indented distad. Post-discal band faintly marked lighter than ground colour. Three submarginal bands (hsm1 to hsm3) clearly marked grey and comprising long dashes between veins, those in hsm2 and hsm3 concave distad. As on forewing, submarginal bands appear to be greyish blue but are pure grey. **Hindwing underside:** Broad whitish band (hb1) along costa extending from base roughly 45% of distance to apex. Two further bands, proximal band (hb2) narrow, distal band (hb3) broad and extending from inner margin curving to follow proximal band. Discal band as upperside but less sharply defined edges to individual marks. Post-discal band series of grey-brown linear marks extending from space 2A to Sc+R1. Three grey-brown submarginal bands well defined, proximal band (hsm1) broadest and distal bands progressively narrowing to hsm3. Proximal two submarginal bands extending from space 2A to space Rs. Distal submarginal band (hsm3) extending from Cu1 to Rs and comprising marks concave distad. Outer margin slightly scalloped as forewing.

Genitalia ♀ (Fig. 24)

Ostium plate comprises thin sclerotised border around ostium bursae, open posterior (not shown in Fig. 24). Well-defined pocket between 7th and 8th tergites and notch midway along ventral edge of 8th tergite.

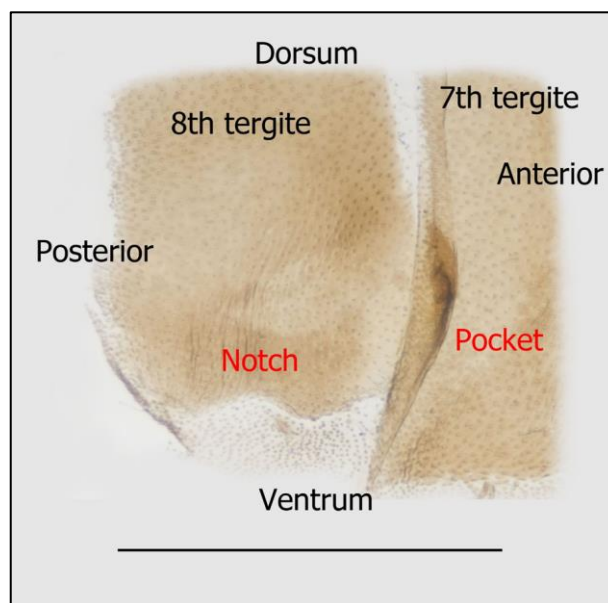


Figure 24 – The 7th and 8th tergites of holotype of *Neptis paulinae* showing pocket and notch typical of Nysiades group species.

Holotype barcode: 658 base pairs,

```
AACTTTATATTTTATTTTGGAAATTTGGGCTGGAATA
GTAGGAACCTTCTCTTAGTTTATTAATTCGAACGAA
TTAGGTAACCCGGGATCTTTAATTGGAGATGATCAA
ATTTATAATACTATTGTAACCTGCTCATGCAATTTATCA
TAATTTTTTTTATAGTTATACCTATTATAATTGGAGG
ATTTGGTAATTGATTAGTTCCTTAATATTAGGAGC
CCCTGACATAGCCTTCCCCTCGAATAAAATAATAAG
ATTTGACTTCTTCCCCTCTTTAATTTTATTAATT
CTAGTAGAATTGTAGAACTGGAGCCGGAACAGGG
TGAACAGTATACCCTCCCTTATCTTCAAACATTGCT
CATGGTGGAGCTTCTGTAGATTTAGCTATTTTTTCTT
TACATTTAGCAGGTATTTCTTCTATTTTAGGGCAA
TTAATTTTATTACAACCTATTATTAATATACGTATTAA
TAATATATCATTTGATCAAATACCTTTATTTGTTTGA
TCAGTGGGAATTACAGCTCTATTACTTTTTATCTT
TACCTGTATTAGCTGGGGCTATTACAATACTTCTAA
CAGATCGAAATTTAAACACCTCATTTTTTGACCCTG
CTGGAGGAGGAGACCCTATCTTTATCAACACTTAT
TT
```

Barcoding

The single specimen of *N. paulinae* yielded a full-length barcode, 658 base pairs, that is allocated to BOLD BIN ADF9273. Several species have smaller barcode pairwise differences with respect to *N. paulinae* than do *N. lugubris* and *N. angelae*, but these are not recovered as close relatives in the multi-gene phylogeny.

Material examined and distribution

The species *N. paulinae* is known from a single female captured near Otto Maber in Nord-Kivu province in the NE DRC. This specimen, the holotype, is in the ABRI collection in Nairobi. The collection locality for the specimen is plotted on the map, Fig. 23, along with collection localities for *N. paulinae* and *N. lugubris*

obtained from the data for specimens in the ABRI collection.

Diagnosis

The holotype female of *N. paulinae* has a broad forewing discal band of near constant width with only the apical section (fd6 and fd7) broadening slightly. This distinguishes the holotype from specimens of other species, such as *N. metanira*, which have a narrower forewing discal band. It is possible that the discal band of the male of *N. paulinae* is narrower leading to a greater risk of confusion with *N. metanira*. The holotype of *N. paulinae* is shown in Fig. 25 together with a barcoded specimen of *N. metanira* to illustrate the potential for misidentification of these two species. The facies of *N. metanira* are variable and the illustrated specimen is chosen from 8 barcoded specimens as the closest in appearance to *N. paulinae*. In Fig. 25 it can also be seen that *N. paulinae* has a slightly more falcate forewing than *N. metanira*. If this trend is borne out by further specimens of *N. paulinae*, it will provide an additional diagnostic character.

N. continuata Holland, 1892 is similar to both the above species and can be separated from them by the more pronounced angle on the proximal edge of the forewing discal band at vein M3

It is worth noting that the barcode apd between these three species provides unambiguous identification:

- *N. paulinae* – *N. metanira* APD = 5.4%
- *N. paulinae* – *N. continuata* APD = 6.2%
- *N. metanira* – *N. continuata* APD = 3.8%

Etymology

The third author is pleased to name both *N. angelae* and *N. paulinae* in honour of his wife Angela Pauline in recognition of her stoic perseverance in the face of endless *Neptis* anecdotes.

Metanira subgroup

Neptis ducarme sp. nov. (Fig. 26)

urn:lsid:zoobank.org:act:D414EF11-27FB-4F94-8568-8647386E79F4

Neptis ducarme and *N. ginettae* were amongst the first species from the Nysiades group to be isolated within the ABRI collection as potential new species. They have a similar arrangement of the forewing discal band markings into three separate groups and the males have two or three veins at the base of the hindwing brightly marked yellow. Subsequent barcoding showed the specimens to fall into two distinct species.

Holotype: ♂ Kasugho, Nord-Kivu, DRC, 00°15' S 29°15' E, (-0.2500°, 29.2500°), 23.viii.2017, R. Ducarme. I. Richardson collection

Paratypes: 4 ♂, 7 ♀: data shown in Table 4

Description of facies

Holotype: ♂ IDR-A01994 (Fig. 26 a, b)

Wingspan: 4.8 cm. **Forewing length:** 2.7 cm. **Antenna-wing ratio:** 0.47.

Head: dark brown and unmarked; palps light grey;

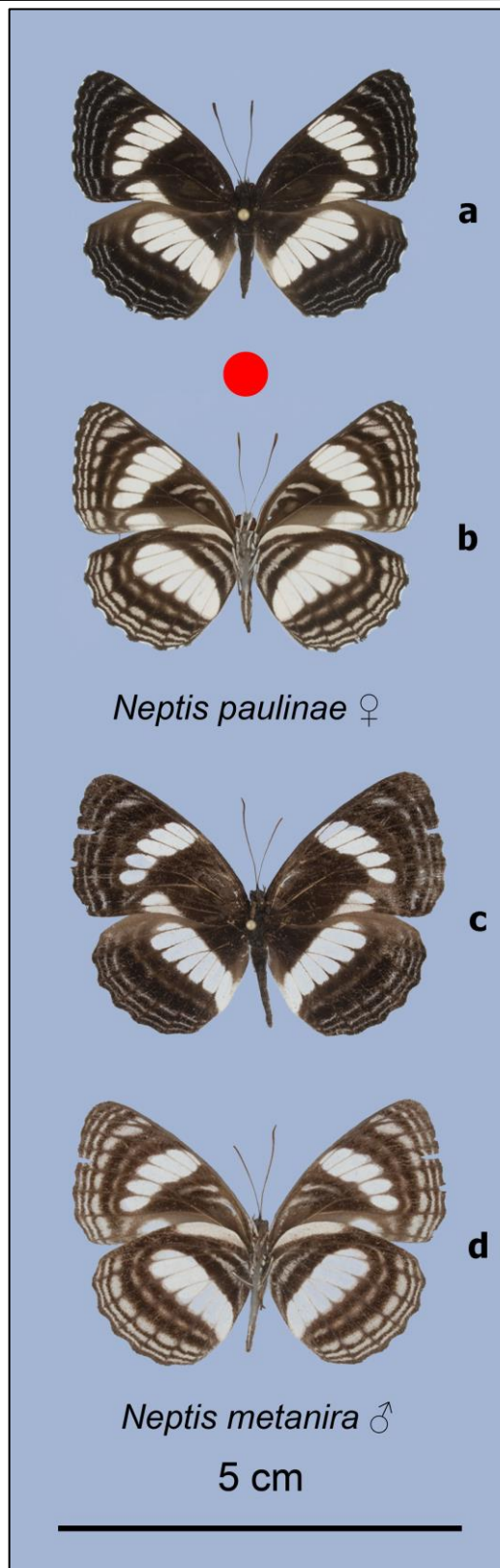


Figure 25 – Comparison of *Neptis paulinae* and *Neptis metanira*. *N. paulinae* holotype ♀: ABRI-162726, Otto Maber, DRC, ix.2016, **a** dorsal, **b** ventral. *N. metanira* ♂: ABRI-162155, Lubango, DRC; vi.2016, **c** dorsal, **d** ventral.

antennae upperside and underside dark grey along entire length.

Thorax: upperside almost black, underside grey-brown. Forelegs, whitish distally mid and hind legs light grey distally.

Abdomen: upperside black, dark grey on underside with

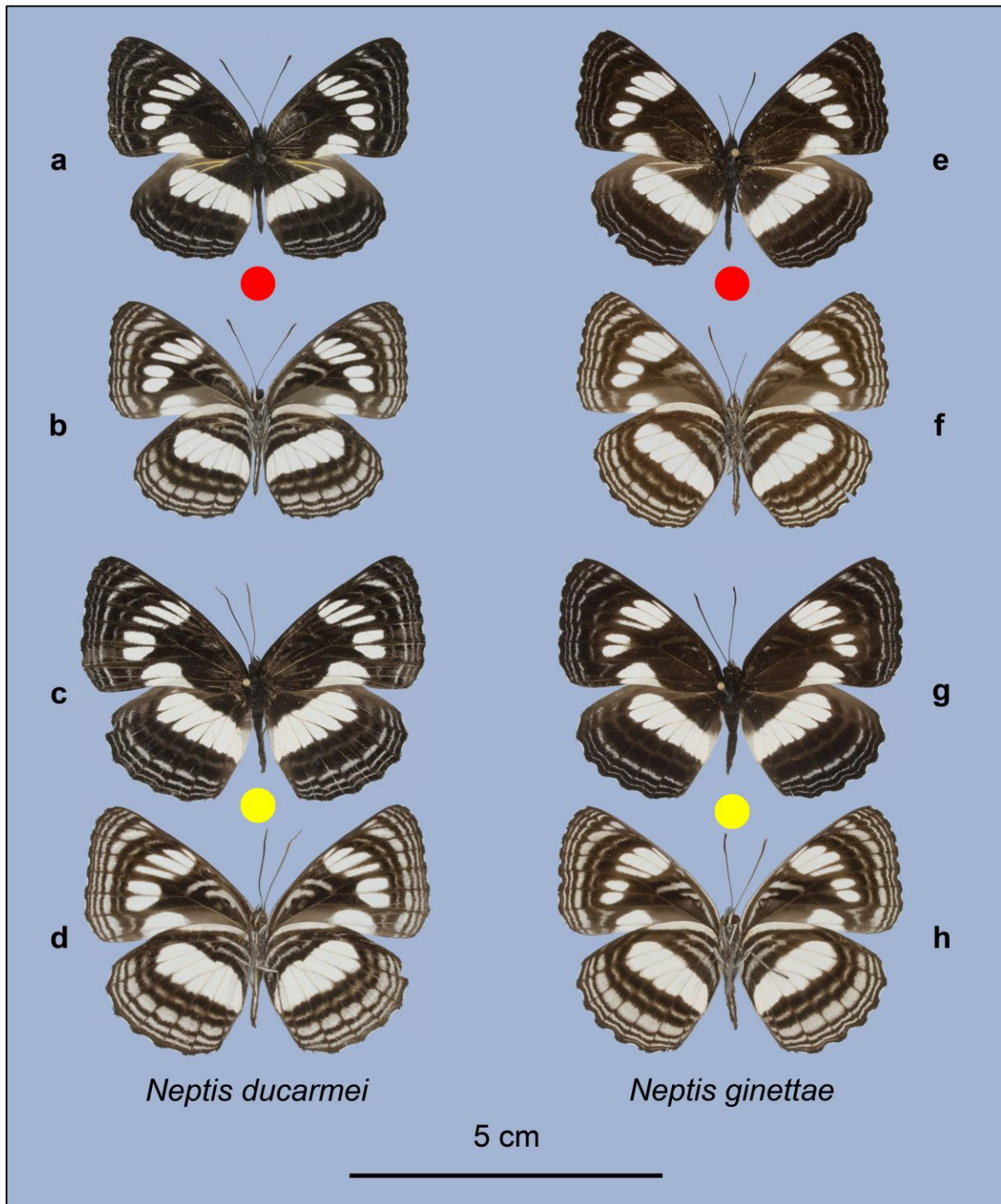


Figure 26 – *Neptis ducarmeii* sp. nov. and *Neptis ginettae* sp. nov. *N. ducarmeii* ♂ holotype: IDR-A01994, Kasugho, Nord-Kivu, DRC, 23.viii.2017, R. Ducarme, **a** dorsal, **b** ventral; *N. ducarmeii* ♀ paratype: ABRI-164703, Lubango, Nord-Kivu, DRC, ix.2016, **c** dorsal, **d** ventral; *N. ginettae* ♂ holotype: ABRI-153000, Kanyasi, Ituri, DRC, i.2015, **e** dorsal, **f** ventral; *N. ginettae* ♀ paratype: ABRI-164706, Kanyasi, Ituri, DRC, i.2015, **g** dorsal, **h** ventral.

continuous whitish ventral line, broad white lateral line.
Wings: Forewing upperside: Background colour black from root to outer margin. Cell unmarked. Discal band markings white from fd1 at inner margin to fd8 at costa. Long discal band mark in space 2A (fd1) ending with rounded point distad and tapering proximad, mark in space Cu2 (fd2) shorter than fd1 tapering distad and with rounded ends, broadly separated (2.0 mm) by background colour from mark in space Cu1 (fd3). Marks in spaces Cu1 and M3 (fd3 and fd4) narrowly separated by background colour proximad and diverging distad. Discal band mark fd5 long and narrow and well separated from fd4, 1.0 mm. fd5

diverging from fd6 distad. Marks fd5 and fd6 longest, fd6 being broader than fd5. fd7 shorter than fd6 and coming to narrow point distad. Final mark fd8 in space R3 shorter again and narrow. At proximal edge of apical section of band fd5 displaced distad relative to fd6 and fd7. Post discal band series of narrow greyish marks and marks in Cu2 displaced proximad relative to line of band from Cu1 to R5. Marks in Cu1 and M2 concave proximad and then mark in R5 linear, final mark in R5 faint and angled proximad at costal end. Three submarginal bands, inner band (fsm1) comprising thin linear marks from space 2A to M1. Mark in R5 longer, more boldly defined, and angled

proximad at costal end. Mark in R4 small and mark in R5 larger. Second submarginal band (fsm2) comprising thin linear marks separated at veins and extending from space 2A to space R3. The outer submarginal band (fsm3) faint and comprising linear marks in spaces Cu2 to R3, faint towards apex. Outer margin with black cilia, indented at veins with patch of white cilia. **Forewing underside:** Ground colour black, spaces 2A and Cu2 lighter greyish, markings white and in same pattern as the upperside but broader. Cell markings comprising radial bar at base (fcr), small spot joined to fcr about halfway along, then broadening at junction with transverse mark fct1. fct1 comprises short thin transverse line. fct1 separated from distal transverse line fct2 by ground colour, fct2 pale brown and broad at costal end, extending across entire cell width. Discal band as upperside but with marks broader and less separated at veins. The postdiscal line series of light grey marks same shape as on upperside but more clearly defined, band indented proximad in space Cu2. Three submarginal bands clearly marked. Proximal band (fsm1) comprises marks in spaces 2A to R3 same shape as on upper side, but much broader and pale brownish grey. Band fsm2 extending from space 2A to space R3 and comprising pale brown marks slightly concave proximad and narrowly separated by veins. Distal band fsm3 similar but not present in space 2A. **Hindwing upperside:** Veins M1, Rs and Sc+R1 pale yellow, first two extending out to discal band. Veins coloured by layer of lamellar scales in somewhat disorganised arrangement, Fig. 27. Broad white discal

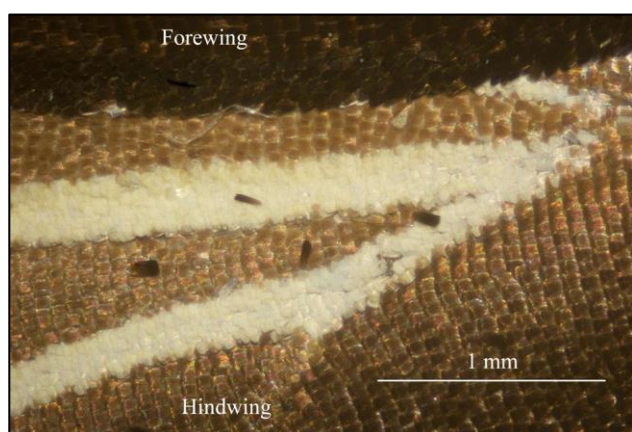


Figure 27 – Photomicrograph showing the pale yellow scales covering veins M1 and Sc+R1 at the base of the hindwing, upperside, of *Neptis ducarme* sp. nov. *N. ducarme* ♂ holotype: IDR-A01994, Kasugho, Nord-Kivu, DRC, 23.viii.2017, R. Ducarme.

band (hd) extending from inner margin in space 2A to space Rs, slightly narrower at inner margin, except for slight extension of mark in space 2A distad, then broadening slightly to hd6 in space M1, ending with shorter mark rounded on anterior edge in space Rs, all marks narrowly separated by ground colour at veins and flat ended distally with some indentation of ground colour along veins Cu1, M1 and M2. Postdiscal line comprises faint mid-brown marks. Three light grey submarginal bands, proximal band (hsm1) well defined with near linear marks, hsm2 and hsm3 comprising narrower lines in each space, hsm1 broadest and hsm3 narrowest. Proximal two submarginal bands extending from space 2A to space Rs where they are faintly defined and distal band extending only to space M1. Outer margin scalloped as forewing, but

with broader patches of white cilia. **Hindwing underside:** Basal line along costa (hb1) brownish white and extending along approximately half of length of costa, second basal line (hb2) pale grey brown, narrow and about half length of hb1, third basal line (hb3) pale brown, well defined from inner margin to space M2, with detached spots in spaces M1 and Rs. Discal band white as on upperside. Postdiscal band extending from inner margin and curving around discal band to space Rs, brownish grey and clearly defined against background colour with lighter scales centrally in spaces 2A to M1. Three submarginal bands comprising of white marks separated at veins. Proximal band (hsm1) broad, narrowing slightly at extremities, extending from inner margin, space 2A, to space Rs. Middle band (hsm2) narrow and comprising slightly curved marks, extending from space 2A to space Rs. Third band (hsm3) similar and extending from space Cu2 to space Rs.

Genitalia ♂: (Fig. 28) Uncus curving ventrad initially then more or less straight for distal half, small hook at the tip. Ventral edge of valve curved at centre, dorsal edge straight from apical process along $\frac{3}{4}$ of length of valve, aspect ratio height/length = 0.28, apical process comprising straight stem terminating in ventral hook turning proximad, ventral closure narrow with rounded end, dorsal process not pronounced, elongated and rounded. Aedeagus short and broad, length ratio relative to valve, A/V = 0.83.

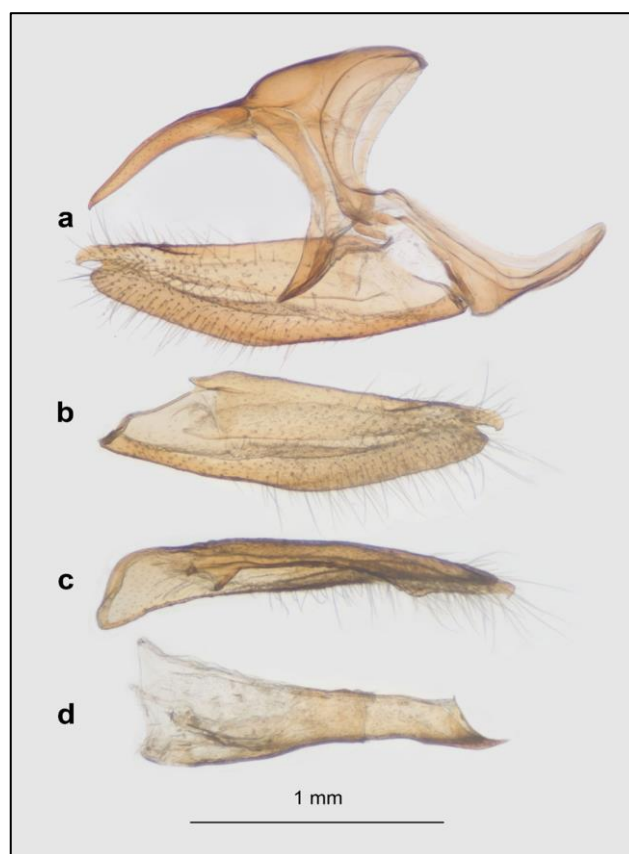


Figure 28 – *Neptis ducarme* ♂ genitalia: ABRI-162699, Otto Maber, Ituri, DRC, ix.2016. **a** genitalia with aedeagus and right valve removed, **b** right valve lateral view, **c** right valve dorsal view, **d** aedeagus lateral view.

Paratype: ♀ ABRI-164703, Lubango, Nord-Kivu, DRC, ABRI collection (Fig. 26 c, d)
Wingspan: 5.6 cm. Forewing length: 3.1 cm. Antenna-
wing ratio: 0.425.

The description below highlights the differences between the holotype and the paratype rather than repeating elements that are almost identical.

Head: Same as holotype

Thorax: Same as holotype

Abdomen: Same as holotype except thin ventral line more clearly defined.

Wings: Forewing upperside: White discal band as in holotype, but the mark fd5 more widely detached from fd6 along its full length and distal submarginal band, fsm3, well defined from space 2A to space R3.

Forewing underside: Similar to holotype except fourth submarginal band (hsm4) faintly marked extending from space Cu1 to space R3 and background colour in spaces 2A and Cu2 darker and not extending to vein Cu2. **Hindwing upperside:** Similar to holotype except veins M1, Rs and Sc+R1 not coloured yellow brown.

Hindwing underside : Same as holotype

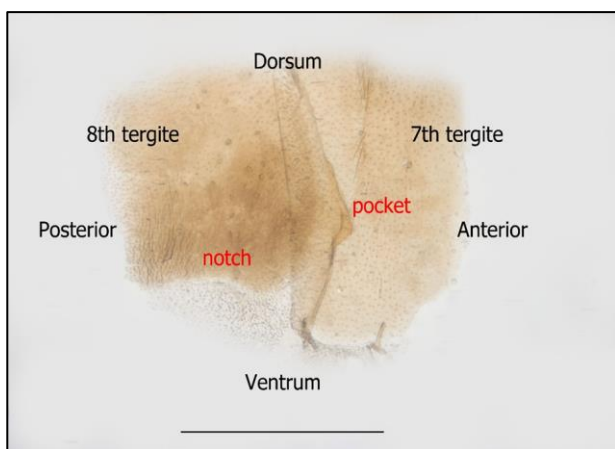


Figure 29 – *Neptis ducarmei* 7th and 8th tergites of the female abdomen. ABRI-164707, Lubango, Nord-Kivu, DRC, x.2014.

Sclerotisation of the abdominal exoskeleton ♀ (Fig. 29) The ostium plate not sclerotised except for a broad band extending round the anterior edge of the ostium bursae, not closed on the posterior edge. A pocket between the 7th and 8th tergites. Notch on the ventral edge of the 8th tergite not discernible.

Holotype barcode: 658 base pairs,

AACTTTATATTTTTATTTTTGGAATCTGAGCTGGAA
TAGTAGGTACATCTCTTAGTTTATTAATTGGA
GAAGTAACTGATCTTTAATTGGAGATG
ACCAAATTTATAATACTATCGTAACTGCCATGC
ATTTATTATAATTTTTTTTTATAGTTATACCTATTA
TAATTGGAGGATTTGGTAATTGACTAGTTCCCTT
AATACTAGGAGCTCCTGACATAGCCTTCCCTCGA
ATAAATAATATAAGATTTTGACTTCTCCCCCTC
TTTAATTTTATTAATTTCTAGAAGAATTGTAGAA
ACTGGAGCCGGAACAGGTTGAACAGTATACCCC
CCTTTATCTTCTAATATTGCCATGGGGGGGCTTC
TGTAAGCTTAGCTATTTTTCTTTACATTTAGCAG
GTATTTCTTCTATTTTAGGAGCAATTAATTTTATT
ACGACTATTATAATATACGTATTAATAATATAT
CATTTGATCAAATACCTTTATTTGTTTGTACTGTG
GGAATTACAGCTTTATGTTACTTCTATCTTTACC
TGATTAGCTGGAGCTATTACAATATTATTAACA
GATCGAAATTTAAATACTTCAATTTTTGACCCTGC
TGGGGGAGGAGATCCTATTCTTTATCAACATTTA
TTT

Barcoding

A total of 13 specimens of *N. ducarmei* have been barcoded, yielding 658 base pair sequences except in one case with a shorter length of only 626 base pairs. The sequences fall into three groups based on their APD relative to the barcodes of other specimens of the species, as can be seen in the Klee diagram, Fig. 30.

Country	Species	DRC	DRC	DRC	DRC	DRC	DRC	DRC	DRC	DRC	DRC	DRC	DRC	DRC	Gabon	DRC	DRC	DRC	DRC	DRC	DRC	DRC			
Country	Species	<i>sobrina</i>	<i>ducarmei</i>	<i>ducarmei</i>	<i>ducarmei</i>	<i>ducarmei</i>	<i>ducarmei</i>	<i>ducarmei</i>	<i>ducarmei</i>	<i>ducarmei</i>	<i>ducarmei</i>	<i>ducarmei</i>	<i>ducarmei</i>	<i>ducarmei</i>	<i>near ducarmei</i>	<i>near ducarmei</i>	<i>near ducarmei</i>	<i>ginettae</i>	<i>ginettae</i>	<i>ginettae</i>	<i>ginettae</i>	<i>ginettae</i>	<i>ginettae</i>	<i>ginettae</i>	
DRC	<i>sobrina</i>	0.0																							
DRC	<i>ducarmei</i>	4.9	0.0																						
DRC	<i>ducarmei</i>	5.1	0.9	0.0																					
DRC	<i>ducarmei</i>	5.1	0.6	0.3	0.0																				
DRC	<i>ducarmei</i>	5.1	0.2	1.1	0.8	0.0																			
DRC	<i>ducarmei</i>	5.2	0.8	0.5	0.2	0.9	0.0																		
DRC	<i>ducarmei</i>	4.9	0.5	0.8	0.5	0.6	0.6	0.0																	
DRC	<i>ducarmei</i>	5.1	0.9	0.6	0.3	1.1	0.5	0.8	0.0																
DRC	<i>ducarmei</i>	5.2	0.8	0.5	0.2	0.9	0.3	0.6	0.5	0.0															
DRC	<i>ducarmei</i>	5.1	0.2	1.1	0.8	0.3	0.9	0.6	1.1	0.9	0.0														
DRC	<i>ducarmei</i>	4.9	0.8	0.5	0.2	0.9	0.3	0.6	0.5	0.3	0.9	0.0													
DRC	<i>near ducarmei</i>	5.1	1.1	1.7	1.4	1.2	1.2	1.2	1.4	1.5	1.2	1.5	0.0												
DRC	<i>near ducarmei</i>	5.4	1.1	1.8	1.5	1.3	1.3	1.3	1.5	1.6	1.3	1.6	0.0	0.0											
Gabon	<i>near ducarmei</i>	3.8	2.5	2.8	2.5	2.6	2.6	2.3	2.8	2.6	2.6	2.6	3.0	3.1	0.0										
DRC	<i>ginettae</i>	5.1	6.7	6.6	6.6	6.6	6.7	6.7	6.6	6.7	6.9	6.7	6.2	6.4	5.7	0.0									
DRC	<i>ginettae</i>	5.2	6.9	6.7	6.7	6.7	6.9	6.9	6.7	6.9	7.1	6.9	6.4	6.6	5.9	0.2	0.0								
DRC	<i>ginettae</i>	5.1	6.7	6.6	6.6	6.6	6.7	6.7	6.6	6.7	6.9	6.7	6.2	6.4	5.7	0.0	0.2	0.0							
DRC	<i>ginettae</i>	5.1	6.9	6.7	6.7	6.7	6.9	6.9	6.7	6.9	7.1	6.9	6.4	6.6	5.9	0.5	0.3	0.5	0.0						
DRC	<i>ginettae</i>	5.1	6.9	6.7	6.7	6.7	6.9	6.9	6.7	6.9	7.1	6.9	6.4	6.6	5.9	0.5	0.3	0.5	0.0	0.0					
DRC	<i>ginettae</i>	5.1	6.9	6.7	6.7	6.7	6.9	6.9	6.7	6.9	7.1	6.9	6.4	6.6	5.9	0.5	0.3	0.5	0.0	0.0	0.0				
DRC	<i>ginettae</i>	5.2	6.9	6.7	6.7	6.7	6.9	6.9	6.7	6.9	7.1	6.9	6.4	6.6	5.9	0.2	0.0	0.2	0.3	0.3	0.3	0.3			

Figure 30 - Klee diagram showing barcode pairwise differences, as percentages of the barcode length, between specimens of *Neptis ducarmei*, *Neptis ginettae* and *Neptis sobrina*.

The first group comprises 10 specimens, all with full length barcodes, that are allocated to BOLD BIN ACU3699. These form the upper left triangle in Fig. 30 and show significant barcode variability within the group with an intra-species APD of 0.6% and maximum APD of 1.1%. No pair out of these 10 specimens has identical barcodes. The details of the specimens giving rise to this first group of sequences are shown in Table 4 with a white background.

The second group comprises two specimens, the details marked with a yellow background in Table 4, have barcodes of lengths 658 and 626 base pairs and are identical over their shared length. These have a barcode APD 1.4% relative to the first group of 10 specimens. The barcode separation between the two groups is only slightly greater than the largest pd within the first group. The female does not differ from the females in the main group

of 10. However, the male has the apical group of marks in the forewing discal band more tapered than those in the main group. It is judged that insufficient evidence exists currently to separate the two groups and these two specimens are considered conspecific with the larger group of 10 specimens. In BOLD, these two barcodes are shown as “within BIN” in the BIN BOLD: ACU3699, in agreement with the specimens being conspecific with *N. ducarmei*.

A third barcode group comprises a single barcode, the specimen details marked with an orange background in Table 4, from Gabon. Fig. 30 shows this barcode to have an APD of 2.7% with respect to the 12 barcodes of specimens from E. DRC. The barcode separation from *N. ducarmei* suggests a separate but closely related species, confirmed by the allocation of this barcode to a different BOLD BIN: AAI313.

Table 4 – Specimens of *Neptis ducarmei* examined, including a specimen from a population in Gabon. Barcode group 1 is the first 10 specimens (no highlight); barcode group 2 is the next two specimens highlighted yellow; and barcode group 3 is the specimen from Gabon.

Accession number	Collection Data				Sex
	Locality	Elevation (m)	Date	Collector/s	
ABRI-152998	Mamove, Nord-Kivu, DRC	1000	ii.2010	ABRI collector	♂
ABRI-160713	Kwokoro, Sud-Ubangi, DRC	400	iv-vi.2016	ABRI collector	♂
ABRI-162199	Kilau, Nord-Kivu, DRC	1900–2150	v.2014	ABRI collector	♀
ABRI-162699	Otto Maber, Ituri, DRC	1050	ix.2016	ABRI collector	♂
ABRI-164291	Lubango, Nord-Kivu, DRC	2100–2250	ix.2016	ABRI collector	♂
ABRI-164703 paratype ♀	Lubango, Nord-Kivu, DRC	2100–2250	ix.2016	ABRI collector	♀
ABRI-164704	Mabungu, Nord-Kivu, DRC	100–1200	xi.2014	ABRI collector	♀
ABRI-164705	Kilau, Nord-Kivu, DRC	1900–2150	iv.2016	ABRI collector	♀
ABRI-164707	Lubango, Nord-Kivu, DRC	2100–2250	x.2014	ABRI collector	♀
IDR-A01994 holotype ♂	Kasugho, Nord-Kivu, DRC	1800	23.viii.2017	R. Ducarme	♂
ABRI-153047	Mamove, Nord-Kivu, DRC	1000	i.2015	ABRI collector	♂
IDR-A02150	Mamove, Nord-Kivu, DRC	1000	6.xi.2017	R. Ducarme	♀
BC-GVW1060	Ivindo NP, Ogooué-Ivindo, Gabon	550	4.xi.2002	G. Vander weghe	??

Material examined and distribution

Twelve specimens of *N. ducarmei* from the DRC have been examined as shown in Table 4. Eleven of these specimens were captured in the eastern DRC, Nord-Kivu and Ituri provinces and a further specimen was captured further West in lowland forest in Sud-Ubangi province. The collection locality elevations show that the species is to be found from lowland forest through to high elevation montane forest at altitudes over 2000 m.

The single specimen from Gabon was captured by Gael Vander weghe in 2002 and the barcode shows it to be close to *N. ducarmei*. Photographs are not available of either the specimen or its genitalia and so its status cannot be reliably determined until further specimens from the region become available. The collection localities of the DRC specimens are shown on the map, Fig. 31.

The wing measurements have been taken from the 10 barcoded specimens where scaled photographs are available. The measurement statistics are as follows:

Males, N=3:

Forewing length: mean 2.9 cm, $\sigma = 0.13$ cm

Wingspan as set: mean 5.2 cm, $\sigma = 0.30$ cm

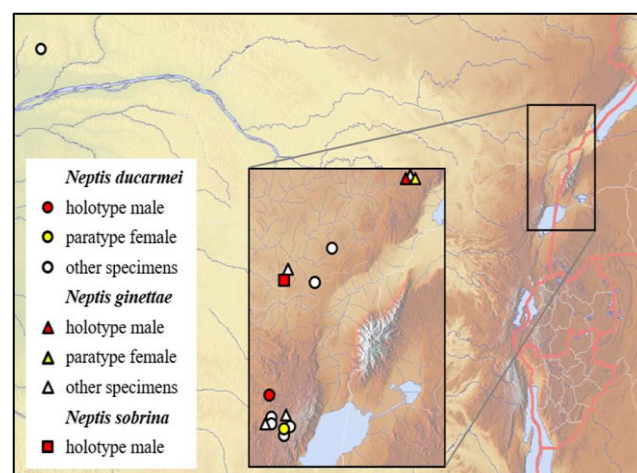


Figure 31 – Capture localities for *Neptis ducarmei*, *Neptis ginettae* and *Neptis sobrina*. All specimens have been barcoded. Note the single specimen of *Neptis ducarmei* shown on the main small scale map far to the West of all the other specimens that were captured in Nord-Kivu and Ituri provinces of the DRC.

Females, N=7:

Forewing length: mean 3.0 cm, $\sigma = 0.09$ cm

Wingspan as set: mean 5.4 cm, $\sigma = 0.15$ cm

Etymology

It is an honour to name *N. ducarme* and *N. ginettae* for Robert and Ginette Ducarme who have collected extensively in the Nord-Kivu and Ituri provinces of the DRC and have made a major contribution to our knowledge of the Lepidoptera of this region, rich in endemic species. They have also sent the third author many *Neptis* specimens for analysis including two of *N. ducarme*, one of which is selected as the holotype.

Diagnosis

The diagnosis for *N. ducarme* is discussed along with the similar *N. ginettae* under the latter species.

Neptis ginettae sp. nov. (Fig. 26)

urn:lsid:zoobank.org:act:E859939D-4C05-429A-9168-EB96B0BB272E

Holotype ♂: ABRI-153000, Kanyasi, Ituri, DRC, 01°35'15" N 30°13'15" E, i.2015, ABRI collection.

Paratypes: 3♂ and 3♀, data shown in Table 2

Description of facies

Holotype: ♂ (Fig. 26 e, f)

Wingspan: 4.8 cm. Forewing length: 2.8 cm. Antenna-wing ratio: 0.46.

Head: Blackish; palps blackish above and light brown grey below; antennae upperside blackish, underside dark reddish brown.

Thorax: Upperside blackish, underside marked greyish/brown. Legs, pale grey distally.

Abdomen: Upperside blackish, underside more greyish with thin continuous light grey ventral line, thin lateral greyish white line.

Wings: **Forewing upperside**: Background colour dark brown. Cell unmarked. White discal band extending from space 2A (fd1) to space R3 (fd8) and comprising three well separated groups of marks; fd1 and fd2 at inner margin, fd3 and fd4 centrally in band, fd5 to fd8 in apical region. Long discal band mark in space 2A (fd1) rounded distad, mark in space Cu2 (fd2) broad, slightly shorter than fd1, rounded anteriorly and distad. Proximal edges of these two marks tapering to form line at approximately 45° to inner margin. Mark fd2 broadly separated (2.0 mm) by background colour from almost triangular mark in space Cu1 (fd3). Mark in space M3 (fd4) elongated with rounded ends and narrowly separated by ground colour along vein Cu1 from fd3. Marks in spaces M3 and M2 (fd4 and fd5) well separated, 1.0 mm, by ground colour along vein M3. Apical section of discal band, marks fd5 to fd8, narrowly separated by veins. fd5 narrow with rounded distal end. fd6 rectangular with flat ends and longest mark in apical group. fd7 same width as fd6 but tapering at distal end. fd8 in space R3 narrow triangular mark pointed distad. Proximal edge of discal band marks fd6 and fd7 flat ended and proximal end of fd5 displaced distad relative to fd6 and fd7. Post-discal band indistinct comprising linear marks, slightly lighter than ground colour, in spaces Cu1 to R5. Two submarginal bands of grey marks in spaces Cu2 to R3, both faint in space 2A at inner margin. The marks in proximal band (fsm1) concave distad in spaces Cu1 to M1, linear in spaces 2A, Cu2 and R5, small and irregular shaped in R4 and R3. The second submarginal band, (fsm2) faint

and comprising linear light grey-brown marks. The outer margin scalloped with broad patch of black cilia at end of veins and narrower patch of white cilia in between.

Forewing underside: Background colour dark brown and lighter than upperside, spaces 2A and Cu2 much lighter. Cell markings light brown comprising thin radial line along anterior edge of cell (fcr) broadening slightly at fcr.1 and broadening again at fct1.1 at root of short and faintly marked transverse line (fct1). After short, unmarked break on anterior edge of cell, second, distal transverse line (fct2) extending across width of cell, fct2 being convex anteriorly and more strongly marked than fct1. Discal band markings white and shaped as on upperside. Post-discal band comprising light brown marks, more clearly defined than corresponding marks on upperside. Three submarginal bands. Proximal submarginal band (fsm1) comprising broad, light brown, linear marks, well separated at veins. A further two submarginal bands (fsm2 and fsm3) clearly marked light brown, largely linear and narrowly separated at veins. The width of submarginal lines reducing from broadest at fsm1 to narrowest at fsm3. Two proximal submarginal bands extending from inner margin to costa. Distal band (fsm3) extending from space Cu2 to costa.

Hindwing upperside: Base of wing dark brown. Spaces Rs, Sc+R1 and h lighter brown. Veins M1 and Rs marked pale yellow out to discal band. Discal band (hd) white, extending from inner margin (hd1) to space Rs (hd7), broadest in space M1 but not tapering significantly at inner margin. The edges of the band linear. The mark hd7 short and convex anteriorly. Individual marks flat ended distad. The band between marks hd4 and hd5 narrowly indented distad, remainder of band not significantly indented distad. Post-discal band faintly marked lighter than ground colour. Three submarginal bands (hsm1 to hsm3) clearly marked light grey and comprising long dashes between veins, those in hsm2 and hsm3 concave distad. Inner submarginal band, hsm1, broadest and width of bands reducing progressively through hsm2 to hsm3. The outer margin scalloped with shorter length of white cilia between longer length of black cilia at ends of veins. **Hindwing underside**: Background colour dark reddish brown, broad light brown band (hb1) along costa extending from base roughly 50% of distance to apex. Two further bands, proximal band (hb2) narrow, distal band (hb3) broad and extending from inner margin curving to follow proximal band. Discal band as upperside. Post-discal band a series of light brown fuzzy curved marks, convex proximally, extending from space 2A to Sc+R1. Three light brown submarginal bands well defined, proximal band (hsm1) broadest and distal bands progressively narrowing to hsm3. The submarginal bands extending from space 2A to space Rs. hsm1 comprising linear marks except that in Cu2 which is convex proximally, hsm2 and hsm3 comprising linear or slightly curved marks convex proximally.

Genitalia ♂ (Fig. 32): Uncus gently curving ventrad with slightly hooked end. Ventral edge of valve curving throughout and more pronounced midway along and dorsal edge almost linear. Aspect ratio width/length 0.29. Apical process short and comprising fine spike without hooks at end. Ventral closure rounded and notch rounded. Apical process substantial structure comprising curved plate extending at right angles to the body of the valve and with the tip turning dorsad. Aedeagus short and broad with apical spike only slightly curved, length ratio relative to

valve, $A/V = 0.96$. Note that length of aedeagus is uncertain owing to damage to proximal end.

Paratype: ♀ (Fig. 26 g, h) ABRI-164706, Kanyasi, Ituri, DRC, 01°35'15" N, 30°13'15" E (1.5875°, 30.2208°), ABRI collection

Wingspan: 5.5 cm. Forewing length: 3.1 cm. Antenna-wing ratio: 0.42.

The description below highlights the differences between the holotype and the paratype rather than repeating elements that are almost identical.

Head: Same as holotype

Thorax: Same as holotype

Abdomen: Same as holotype

Wings: Forewing upperside: Cell showing underside markings faintly. White discal band as in holotype, except slightly more indentation at veins on distal edge. Mark fd5 narrower than in holotype and angled away from fd6 distad. Postdiscal band more clearly marked than in holotype and forming a triangular indentation between marks fd2 and fd3. Submarginal bands fsm1 and fsm2 similar to holotype, but more clearly defined with more linear marks throughout in place of curved marks of holotype in fsm1. A third submarginal band clearly defined with long linear marks between veins. **Forewing underside:** Generally as in holotype except radial line in cell, fcr, broader and transverse lines fct1 and fct2 more solidly defined. Submarginal fsm1 broader than in holotype, fsm2 broader and comprising curved marks concave proximad in spaces R4 and R5, fsm3 more clearly defined, fsm4 present (not in holotype male) and faintly defined from space Cu1 to space R3. **Hindwing upperside:** As holotype with fsm1 broader than in holotype, veins Rs and Sc+R1 faintly marked lighter than background colour, but not pale yellow. **Hindwing underside:** Markings bolder than in holotype, especially hsm1 much broader. A faintly marked fourth submarginal band, hsm4, from space Cu2 to space M3.

Genitalia: ♀ (Fig. 33) The ostium plate not sclerotised except for a broad band extending round anterior edge of ostium bursae, not closed on posterior edge. A pocket between 7th and 8th tergites. Deep notch on ventral edge of 8th tergite.

Holotype barcode: 658 base pairs,
TAC TTTATATTTTATTTTGGGAATCTGAGCTGGAATA
GTGGGCACATCTCTTAGCTTATTAATTCGATCTGAA
TTAGGTAACCCAGGATCTTTAATTGGGGATGATCAA
ATTTATAATACTATTGTAAGTCTCATGCATTTATTA
TAATTTTTTTCATAGTTATACCTATTATAATTGGAGG
ATTTGGTAATTGACTGGTCCCTTTAATATTAGGAGC
CCCTGATATAGCTTTCCCTCGAATAAATAACATAAG
ATTTTGACTTCTTCCCCCTCTTTAGTTTTGTTAATTT
CTAGTAGAATTGTAGAACTGGGGCCGGAACAGGA
TGAACAGTATACCCTCCACTTCTTCAAATATTGCTC
ATGGGGGGCTTCTGTAGATTTAGCTATTTTTCTTT
ACATTTAGCGGGTATTTCTTCTATTTTAGGGGCAAT
TAATTTTATTACAATATTATTAATATACGAATTAA
TAATATATCATTTGATCAAATACCTTTATTTGTTTGA
TCAGTAGGAATTACAGCTTTATTGTTACTCTTATCTT
TACCAGTATTAGCTGGAGCTATTACAATATTATTA
CAGATCGAAATTTAAATACTTCATTTTTTGACCCAG
CTGGAGGGGGAGACCCTATTCTTTACCAACATTTAT
TT

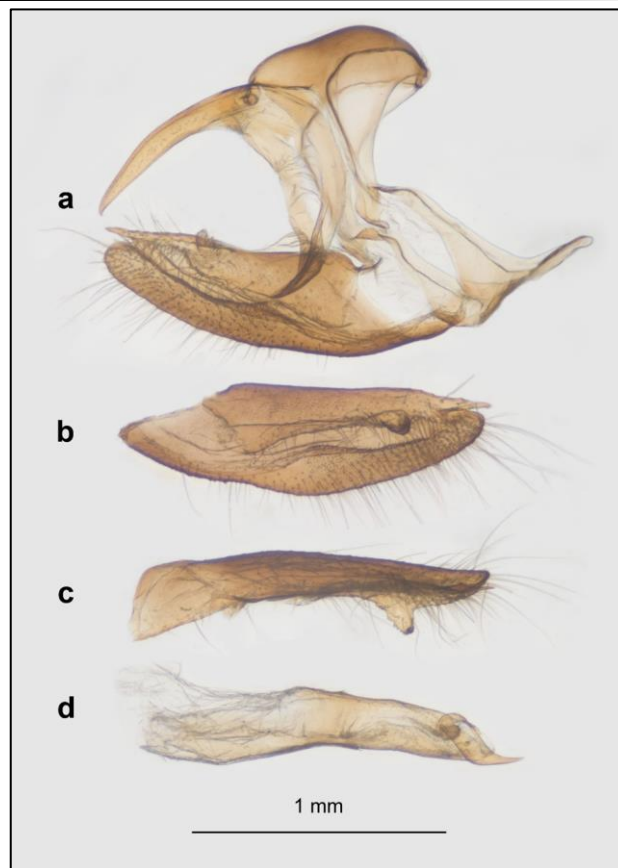


Figure 32 – *Neptis ginettæ* male genitalia: ABRI-164047, Kilau, Nord-Kivu, DRC, ii.2016. **a** genitalia with aedeagus and right valve removed, **b** right valve lateral view, **c** right valve dorsal view, **d** aedeagus lateral view.

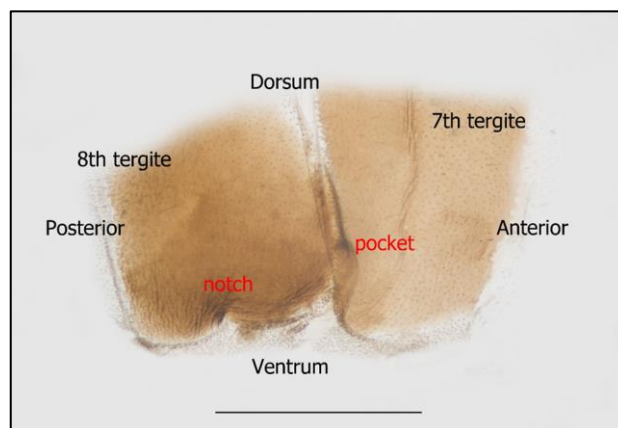


Figure 33 – *Neptis ginettæ* 7th and 8th tergites of the female abdomen. ABRI-164706, Kibale, Nord-Kivu, DRC, ii.2016.

Barcoding

Seven specimens of *N. ginettæ* yielded full length barcodes, 658 base pairs, that are allocated to BOLD BIN ACU3626. These seven barcodes have low variability with an intraspecific APD of 0.25% and a maximum APD of 0.5% (3 base pairs).

Material examined and distribution

Five of the barcoded specimens of *N. ginettæ* were collected in mid-elevation forest, (850–1200 m) in Ituri province and three in high elevation forest (1800–2100 m) in Nord-Kivu province in the NE DRC The collection

localities for the seven specimens are plotted on the map (Fig. 31) and the capture data for the eight specimens are listed in Table 5. Although all eight specimens were captured in Nord-Kivu and Ituri provinces, the presence of *N. ginettae* at Manzumbu, 850 m, suggests that the species could also be found more widely across the DRC in low elevation forest.

The wing measurements derived from barcoded specimens are as follows:

Males, N=4:

Forewing length: mean 2.8 cm, $\sigma = 0.05$ cm

Wingspan as set: mean 4.9 cm, $\sigma = 0.09$ cm

Females, N=3:

Forewing length: mean 3.0 cm, $\sigma = 0.04$ cm

Wingspan as set: mean 5.4 cm, $\sigma = 0.17$ cm

Diagnosis

Several morphological features of these two species need

Table 5 – Specimens of *Neptis ginettae* examined.

Accession number	Collection Data			Collector/s	Sex
	Locality	Elevation (m)	Date		
ABRI-150644	Manzumbu, Ituri, DRC	850	vii.2014	ABRI collector	♂
ABRI-150675	Kithokolo, Nord-Kivu, DRC	1900–2100	vi 2014	ABRI collector	♀
ABRI-152984	Kanyasi, Ituri, DRC	1200	i.2015	ABRI collector	♂
ABRI-153000	Kanyasi, Ituri, DRC	1200	i.2015	ABRI collector	♂
ABRI-161282	Kasuo, Nord-Kivu, DRC	1800–1900	i.2016	ABRI collector	♀
ABRI-152985	Kanyasi, Ituri, DRC	1200	i.2015	ABRI collector	♂
ABRI-164706	Kanyasi, Ituri, DRC	1200	i.2015	ABRI collector	♀
ABRI-164047	Kilau, Nord-Kivu, DRC	1900–2150	ii.2016	ABRI collector	♂

A specimen that passes all these tests can be assigned to *N. ducarmeii*, *N. ginettae* or the as-yet-undescribed *N. species13*.

Neptis ginettae can be separated by the form of the apical section of the forewing discal band where fd5 to fd7 form a contiguous, almost rectangular, group with the veins only narrowly marked. This contrasts with the other two species where the apical group is more widely separated by ground colour. It should be noted that one barcoded specimen of *N. ginettae* has the mark fd5 well separated from fd6 distally, whilst fd6 and fd7 are contiguous with the vein M1 only marked by a narrow line.

Intraspecific variability presents a great problem for identification of some species within the Nysiades group and an instance of this is provided by the female of *N. ducarmeii* shown in Fig. 34. This specimen barcodes as *N. ducarmeii*, but the apical group fd5 to fd7 clearly fails test 6 above.

The undescribed *N. species13* closely resembles *N. ducarmeii*, although it is generally slightly smaller, and the male lacks the yellow veins at the base of the hindwing upperside. Fig. 35 shows a male specimen from Cameroon that just meets the size criterion for test 1 above. Note the lack of colouring on the veins of the hindwing upperside. In cases of uncertainty, the barcodes separate *N. species13* from *N. ducarmeii* unambiguously with an APD of 7.4% for 5 barcodes of *N. species13* compared with 12 of *N. ducarmeii*.

to be examined to separate *N. ducarmeii* and *N. ginettae* from other species and from each other. This process constitutes a series of tests concluding with a small number of possible identifications of a specimen that passes all the tests.

1. ♂ wing length > 2.7 cm and wingspan > 4.8 cm, or ♀ wing length > 2.9 cm and wingspan > 5.2 cm (The wing length and wingspan criteria are derived from the mean minus 1 σ).
2. Forewing cell underside showing a radial bar and two transverse bars, not multiple spots. This eliminates *N. constantiae* Condamin, 1966, and the forest form of *N. alta* which have a similar form of discal band.
3. Forewing cell upperside unmarked.
4. Forewing discal band broadly broken by ground colour between fd4 and fd5.
5. Forewing discal band marks fd3 and fd4 only narrowly separated by ground colour.
6. Length of forewing discal band marks fd5 to fd7 nearly equal.

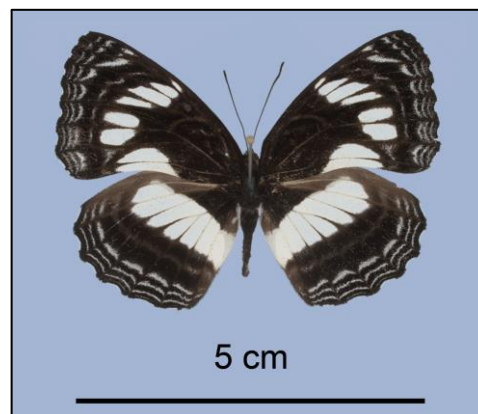


Figure 34 – *Neptis ducarmeii*, variability of the facies ♀: ABRI-164291, Lubango, Nord-Kivu, DRC, ix.2016.

Neptis sobrina sp. nov. (Fig. 36)

urn:lsid:zoobank.org:act:9540BAEB-B1BD-4D4E-AF4B-FF55643958ED

This species is known from a single barcoded male captured in Nord-Kivu province, NE DRC.

Holotype: ♂ Kithokolo, Nord-Kivu, DRC, 01°10' S, 29°13' E, (-1.1667°, 29.2167°); vi.2014, ABRI collection.

Paratypes: None

Description of facies

Holotype: ♂ ABRI-150683 (Fig. 36 a, b)

Wingspan: 4.4 cm. Forewing length: 2.5 cm. Antenna-wing ratio: unknown.

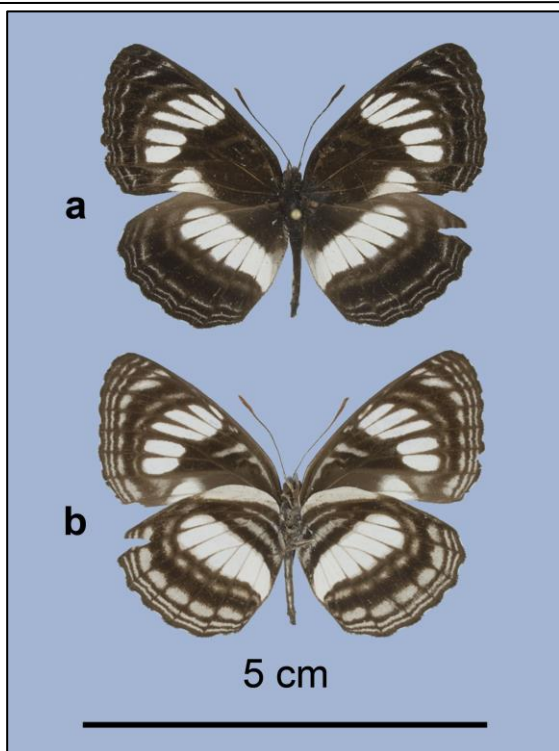


Figure 35 – *Neptis* species13: a large example that could easily be confused with *N. ducarme*. ♂: ABRI-152997, Mecalat, South, Cameroon, iv.2013, ABRI collection.

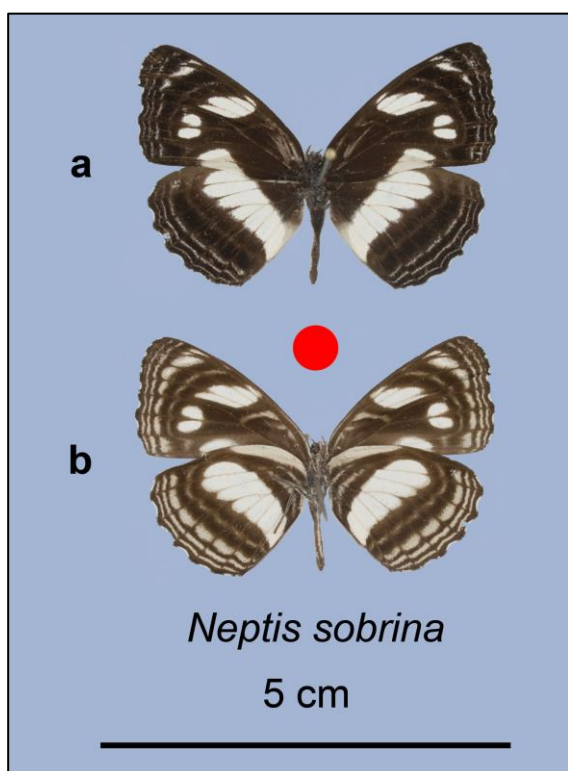


Figure 36 – *Neptis sobrina* sp. nov. Holotype ♂: ABRI-153052, Mapimbi, Ituri, DRC, ix.2014, **a** dorsal, **b** ventral.

Head: Blackish; palps dark above light brown/grey below; antennae missing.

Thorax: Upperside blackish, underside dark brown. Legs, grey distally.

Abdomen: Upperside blackish then more greyish distad, a continuous light grey ventral line and thin light grey lateral lines.

Wings: Forewing upperside: Background colour dark brown to black at apex, grading to a slightly lighter shade at base. Cell unmarked. Discal band composed of white marks extending from space 2A at inner margin to space R3 at costa and comprising three well separated groups; fd1 and fd2 at inner margin, fd3 and fd4 forming middle group, fd5 to fd8 in apical region and displaced proximad relative to middle group. Elongated discal band mark in space 2A (fd1) tapering to blunt point distad and with flat angled proximal end, mark in space Cu2 (fd2) broad, slightly shorter than fd1 and tapering to point distad. Proximal edges of these two marks forming line at approximately 45° to inner margin. Mark fd2 broadly separated (2.3 mm) by background colour from mark in space Cu1 (fd3). Mark fd3 elliptical and only narrowly separated from fd4. fd4 shorter and well separated (1.1 mm) from fd5 by ground colour. Apical marks fd5 to fd7 longer and almost contiguous only narrowly separated by veins, fd5 and fd6 longest with fd5 narrow and fd6 broad. fd8 long thin linear mark in space R3. The proximal edge of discal band marks fd5 to fd7 flat ended and fd5 strongly tapered distad. Proximal edge of marks fd5 to fd7 linear or slightly convex proximad. Faintly marked post-discal band comprising indistinct brownish marks in spaces Cu2 to R5 except fsm3 terminating in space R4. fsm1 comprising linear or slightly curved marks, then in space M1 more brightly defined mark, in space R5 larger wedge-shaped mark, in space R4 small indistinct mark and finally in space R3 and narrow triangular mark parallel to costa. Outer submarginals comprising narrow curved line segments, proximally convex. Outer margin scalloped with broad patch of black cilia at end of veins and narrow patch of white cilia in between. **Forewing underside** Background colour dark brown and lighter than upperside, spaces 2A and Cu2 much lighter. Cell markings greyish-brown comprising faint greyish radial line along anterior edge of cell (fcr) broadening at fcr.1 and broadening again at fct1.1 at root of short and faintly marked transverse line (fct1). After short, unmarked break on anterior edge of cell, second, distal transverse line (fct2) extending across entire width of cell, fct2 being convex anteriorad and more strongly marked than fct1. Discal band markings creamy white as on upperside, but less sharply defined at edges. Post-discal band comprising greyish-brown marks, more clearly defined than on upperside, marks linear and mark in Cu2 displaced proximad. Proximal submarginal band (fsm1) comprising broad, light brown, linear or slightly curved marks, broadly separated at veins. Further two submarginal bands (fsm2 and fsm3) clearly marked light brown, linear and more narrowly separated at veins. Width of submarginal lines reducing from broadest at fsm1 to narrowest at fsm3. Three submarginal bands extending from inner margin in space Cu2 to costa in space R3. Fourth submarginal band, fsm4, faintly defined in spaces M1 and R5. **Hindwing upperside** Base of wing ground coloured without any markings. Discal band (hd) white, extending from inner margin (hd1) to space Rs (hd7), broadest in space M1 (hd6), tapering to inner margin where mark hd1 extends distally along inner margin. Mark hd7 short and convex anteriorad. Individual marks hd1 to hd6 flat ended distad or rounded. Post-discal band faintly marked lighter than ground colour. Three submarginal bands (hsm1 to hsm3) clearly marked light brownish-grey and

comprising long linear dashes between veins. Outer margin scalloped with tufts of black scales at end of veins and white cilia in between. **Hindwing underside** Broad whitish band (hb1) along costa extending from base roughly 45% of distance to apex. Two further bands, proximal band (hb2) narrow and short, distal band (hb3) broader and extending from inner margin curving to follow proximal band through to space M1. Discal band white as upperside. Post-discal band series of light brown linear marks extending from space 2A to space Rs. Three pale brown submarginal bands well defined, proximal band (hsm1) broadest and distal bands progressively narrowing to hsm3. Proximal two submarginal bands extending from space 2A to space Rs. Distal submarginal band (hsm3) extending from Cu2 to Rs.

Genitalia: ♂ (Fig. 37): Uncus curving uniformly ventrad with hooked tip. Ventral edge of valve curving from ventral closure to mid-point, broadest point of valve, then curving convex. Dorsal edge curving from base of apical process about $\frac{2}{3}$ of length of valve. Stem of apical process angled dorsad relative to dorsal edge of valve. Form of terminal structure of apical process unknown as this has been broken off both valves. Aspect ratio height/length = 0.27. Dorsal process an elongated triangular shape. Aedeagus short and broad, length ratio relative to valve, A/V = 0.90.

Holotype barcode: 658 base pairs,

```
AACTTTATATTTTATTTTTGGAATTTGAGCTGGAA
TAGTAGGTACATCTCTTAGTTTATTAATTCGAACT
GAATTAGGTAATCCAGGATCTTTAATTGGGGATG
ATCAAATTTATAATACTATTGTAAGTCTCATGC
ATTTATTATAATTTTTTTTATAGTTATACCTATTA
TAATTGGAGGATTTGGAAATTGACTAGTCCCTTT
AATATTAGGAGCCCCTGATATAGCTTTCCCCCGA
ATAAATAATATAAGATTTTGACTTCTCCCCCCTC
TTTAATTTTATTAATTTCTAGTAGAATTGTAGAAA
CTGGAGCCGGAACAGGATGAACGGTATACCCCC
CCTTATCTTCAAATATTGCCCATAGAGGAGCTTC
TGTAGATTTAGCTATTTTTCTTTACATTTAGCAG
GTATTTCTTCTATTTTAGGAGCAATTAATTTTATT
ACAATATTATTAATATACGTATTAATAATATAT
CATTGATCAAATACCTTTATTTGTTTGATCAGTA
GGAATTACAGCTTTATTACTTCTATCTTTACC
AGTATTAGCTGGAGCTATTACAATATTATTAACA
GATCGAAATTTAAATACTTCATTTTTTGATCCTGC
TGGAGGAGGAGATCCTATTCTTTACCAACATTTA
TTT
```

Barcoding

The single specimen of *N. sobrina* yielded a full length barcode, 658 base pairs, that is allocated to BOLD BIN ACU3871. An unusual feature of the barcode is that it is close, APD < 5%, to that of 15 other species in the Nysiades group.

Material examined and distribution

The single known specimen of *N. sobrina* was collected in high elevation forest at Mapimbi in Ituri province in the NE DRC. The collection locality for the holotype specimen is plotted on the map (Fig. 31).

Etymology

The name *N. sobrina* is taken from the Latin *sobrina*

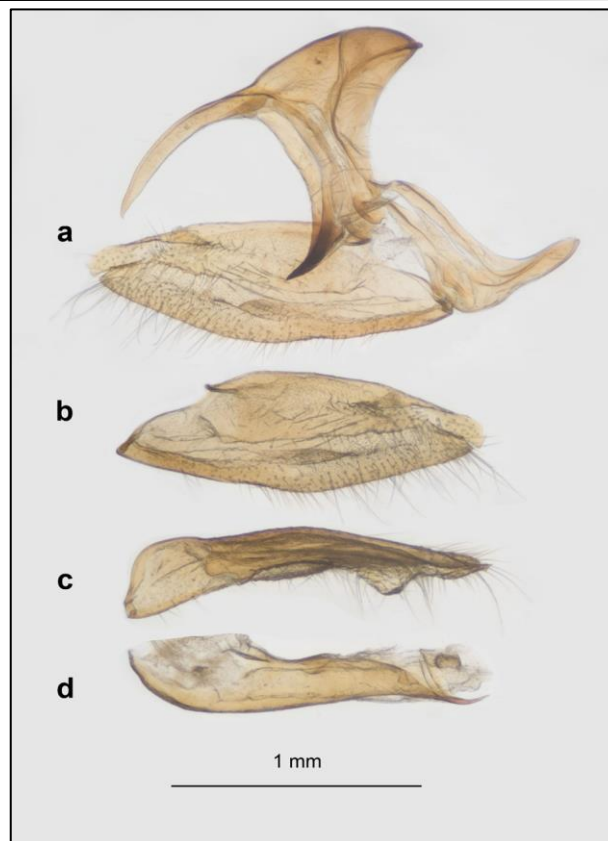


Figure 37 – *Neptis sobrina* male genitalia. Holotype ♂: ABRI-153052, Mapimbi, Ituri, DRC, ix.2014. **a** genitalia with aedeagus and right valve removed, **b** right valve lateral view, **c** right valve dorsal view, **d** aedeagus lateral view.

meaning cousin, reflecting the apparent close relationship of this species with many other species in the Nysiades group as implied by the barcode.

Diagnosis

This species is smaller than *N. ducarme* and *N. ginettae* and is unlikely to be confused with those two species owing to the displacement proximad of the apical portion of the forewing discal band. In fact, this positioning of the marks fd5 to fd7 relative to the central pair fd3 and fd4 is uncommon amongst species in the Nysiades group. Only two undescribed species, currently designated *N. species11* and *N. species11b*, have a similar discal pattern.

The forewings on the three similar species are shown in Fig. 38, scaled x2 when viewed on the A4 page. Several features distinguish these species:

1. The forewing of *N. sobrina* is noticeably narrower than that of the other two species. Quantifying the forewing width as the distance, W, from the apex to the inner margin along a line parallel to the axis of the body normalised by the wing length, L, we obtain: W/L = 0.58 for *N. sobrina*, 0.66 for *N. species11*, 0.68 for *N. species11b*.
2. The apical group of marks in the forewing discal band of *N. sobrina* comprises fd5 narrow, fd6 broad, fd7 narrow and short. This contrasts with fd5 and fd6 long and broad, fd7 narrow and short in *N. species11*, where fd7 is missing in some specimens. For *N. species11b*, fd5, fd6 and fd7 are all broad and of equal length. These differences are seen in all barcoded specimens of the

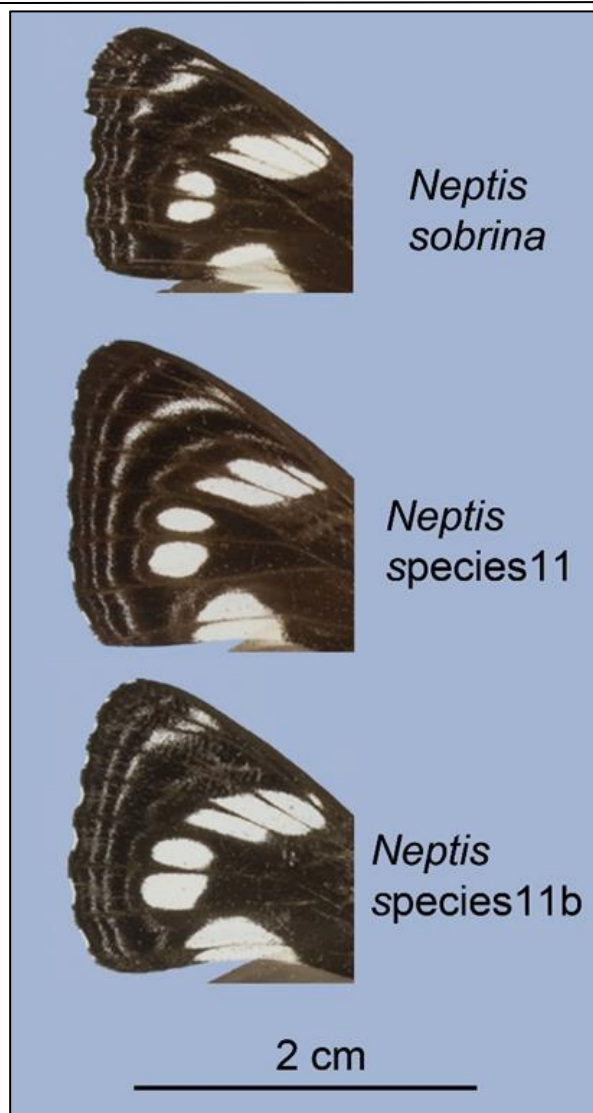


Figure 38 – Forewings of *Neptis sobrina* and two undescribed species with similar wing patterns. *Neptis sobrina* ♂: ABRI-153052, Mapimbi, Ituri, DRC, ix.2014; *Neptis species11* ♂; IDR-A02180, Mamove, Nord-Kivu, DRC, 8.x.2017, R. Ducarme; *Neptis species11b* ♂; IDR-A02025, Mamove, Nord-Kivu, DRC, 9.viii.2017, R. Ducarme.

three species.

3. The central marks, fd3 and fd4, are smallest in *N. sobrina* and largest in *N. species11b*.
4. The form of the apical marks of the inner submarginal band, fsm1, differs between the three species. In *N. sobrina* the mark in space R5 is in the form of a wedge with the tail curved distad. In *N. species11* it is a long thin line strongly curved proximad at the anterior end. In *N. species11b* it is either a short, curved line or more of a wedge shape with the narrow end proximad.

While these four characters should be sufficient to distinguish the three species, only a single specimen of *N. sobrina* is known to date and variability within the species cannot be assessed. When a good series of *N. sobrina* becomes available and variability can be quantified, it could be that some of the distinguishing characters above are found to be invalid.

The barcode remains a reliable means of distinguishing these three species with interspecific APD as follows:

N. sobrina APD with respect to *N. species11* = 6.0%

N. sobrina APD with respect to *N. species11b* = 4.3%

DISCUSSION

Phylogeny

The multigene phylogeny, Fig. 4, provides the first reliable inference of the relationships among species in the Nysiades group. Nysiades is a species rich group that may comprise as many as 80 species and is by far the largest group of Afrotropical *Neptis*.

The value of understanding the relationships among species is already demonstrated in this paper where three sub-groups each comprising three closely related species are described. In all three groups one species has different facies from the other two:

- *N. kupe* differs markedly from *N. jamesi* and *N. nanciae*
- *N. lugubris* differs markedly from *N. angelae* and *N. paulinae*
- *N. sobrina* differs markedly from *N. ducarme* and *N. ginettae*

Conversely, we see that *N. kupe* and *N. lugubris*, that have similar facies, are in fact quite distantly related within the Nysiades group.

Wing pattern similarity among these distantly related species suggests that they may comprise a mimicry ring in which natural selection by predators has led to their morphological convergence. However, there is no evidence that *Neptis* are unpalatable or aposematic.

As more data on food plants becomes available, it may be possible to determine whether any species are likely to be unpalatable. Currently, there is insufficient knowledge of these taxa to hypothesize that some species are chemically defended.

It is recommended that further species description within the Nysiades group is supported by an updated multigene phylogeny so that relationships can be better understood.

Structure of the valves of the male and tergites of the female

The dissections shown in this paper illustrate morphological structures that are common to many species within the Nysiades group.

In the majority of Nysiades group species, the apical process of the male valve terminates with one or two hooks angled proximad. Additionally, the valves have a dorsal process in the form of a projection on the proximal side of the dorsal fold a short distance from the apical process. The shape and size of these structures varies from species to species and in the case of *N. ginettae*, for example, the apical process lacks any hooks.

In the females there is an elongated sclerotised pocket between the 7th and 8th sternites and a notch midway along the ventral edge of the 7th tergite. These structures are present in many species within the Nysiades group but are absent or replaced by different structures in the other groups within the Afrotropical *Neptis*. Specimens in the

Saclava, Incongrua and Woodwardi groups, as defined by Richardson (2019), have spine receptacles on the 7th tergite, but these are quite different from the pocket seen in the Nysiades group species.

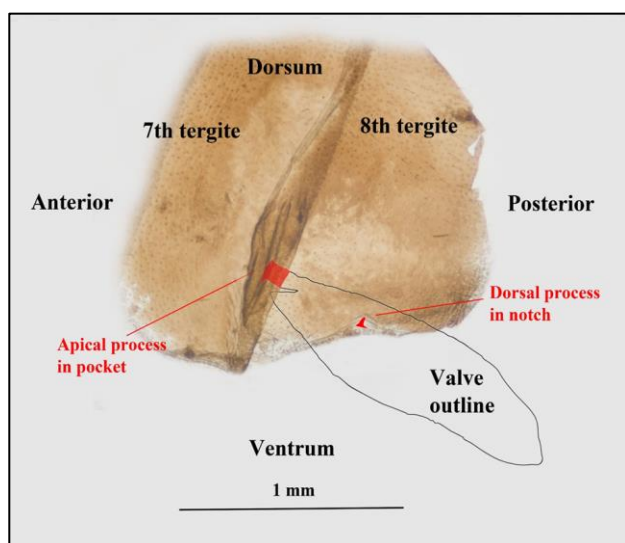


Figure 39 - The location of the valve of male of *Neptis lugubris* with the 7th and 8th tergites of the female. ♂: ABRI-160709, Kanyambia, DRC, vi.2014; ♀: ABRI-160708, Kanyambia, DRC, vi.2014.

Males and females of *N. lugubris* have been dissected and the valve and tergites are superimposed in Fig. 39. The tergites of the female abdomen are shown as a photomicrograph and the valve is shown as an outline traced from another photomicrograph. The scale of the valve has been maintained during the tracing process. The distance between the dorsal process and apical process of the valve matches the distance between the notch on the ventral edge of the 8th tergite and the sclerotised pocket between the tergites. This is strong evidence that the male positions itself during copulation with the dorsal process located in the notch and the apical process tucking into the pocket. This is the positioning shown in Fig. 39 and the two processes locating with the tergites are highlighted in red.

In several of the illustrations of the 7th and 8th tergites in this paper, the pocket is shown clear of both tergites. This is likely to be due to either distention of the abdomen of the gravid female or simply the tergites drifting apart during dissection. In these examples it is not possible to confirm the valve location process as the distance between the notch and the pocket has become much greater than it would have been when the female initially mated.

The apical process is broad in the vertical plane and thin laterally allowing it to fit easily into the pocket. The pocket is long in the vertical direction allowing rotation of the valve without the apical process disengaging from the pocket. The small hooks at the end of the apical process might engage with the sides of the pocket to help maintain the required position of the male relative to the female during copulation. Such a positive location of the valve in the pocket could be difficult to break resulting in the tip of the apical process breaking off when the pair disengage. This would explain why the tip of the apical process is sometimes broken off in males of Nysiades group species.

The definition of the notch on the 8th tergite tends to

correspond with the size of the dorsal process on the valve. *N. ginettae* provides an example of a well-defined notch (Fig. 33) that corresponds to a large dorsal process on the valve (Fig. 32). In this example the apical process lacks hooks and so the effectiveness of the clasping function relies entirely on the large dorsal process engaging in the notch. Conversely, in *N. ducarmei* the notch is poorly defined and corresponds to the dorsal process with a low profile. In this case the clasping function would rely on the hooked apical process engaging in the pocket between the 7th and 8th tergites.

Androconia patches on the hindwings

Two of the new species described in this paper, *N. ducarmei* and *N. ginettae*, have the veins M1, Rs and Sc+R1 at the base of the hindwing upperside prominently marked pale yellow. The photomicrograph (Fig. 27) shows that these markings are due to pale yellow lamellar scales along the veins. The pale yellow scales are in a disorganised and denser arrangement than the background scales, which are arranged in regular lines.

Only four other described species display these pale yellow veins prominently and the full list of species with pale yellow hindwing veins is:

- *Neptis kiriakoffi* Overlaet, 1955, in the Agatha group
- *Neptis constantiae* Carcasson, 1961, in the Agatha group
- *Neptis agouale* Pierre-Baltus, 1978, in the Melicerta group
- *Neptis liberti* Pierre & Pierre-Baltus, 1998, in the Nysiades group
- *Neptis ducarmei* sp. nov., in the Nysiades group
- *Neptis ginettae* sp. nov., in the Nysiades group

In the case of *N. liberti*, the background scales form a silvery oval shape centred on veins M1 and Rs – see Richardson (2019) Fig. 167 on page 146. The yellow veins overlay the silvery patch and have the same disorganised arrangement of scales as in the other five species above.

An excellent, and much reused, photomicrograph of the basal area of the hindwing upperside of *Bicyclus anynana* (Butler, 1879) by Gilles San Martin shows two patches of androconia, see Fig. 40. The left-hand patch comprises tubelike or piliform androconia and the right-hand patch comprises lamellar androconia. The latter are similar in appearance to the scales covering the hindwing veins of the *Neptis* species listed above. It is concluded therefore that these pale-yellow hindwing scales should be called lamellar androconia in the Afrotropical *Neptis*.

Androconia and other specialised scales are thought to disperse pheromones to attract a mate. These can be hair-like tufts, dull or raised patches on the wing, or specialised pockets of the sclerotized wing membrane (Boppré & Vane-Wright, 1989; Darragh *et al.*, 2017, Valencia-Montoya *et al.*, 2021). Chemical characterisation of these putative pheromones is challenging because the active compounds are produced in miniscule amounts. However, several recent studies have identified the active compounds from several species (Bacquet *et al.*, 2015, Darragh *et al.*, 2017, Yoshimori *et al.*, 2022) and determined the genomic basis for the biosynthesis of some pheromone components



Figure 40 – Photomicrograph taken by Gilles San Martin of the basal area of the hindwing upperside of *Bicyclus anynana* showing the androconial spot. The image is reused under the licence Creative Commons Attribution-Share Alike 2.0 Generic.

(Byers *et al.*, 2020, Cama *et al.*, 2022).

However, recent research indicates that androconia may not always be associated with pheromones. Dr Oskar Brattström (personal discussion) kindly updated me on recent research results from his work at the University of Cambridge on *Bicyclus* species, showing that whilst most pheromones in this genus are produced in the androconial patches and brushes, many of these structures are not showing any chemical activity at all (see also Bacquet *et al.*, 2015). Furthermore, when species pairs of *Bicyclus* that have different androconial configurations are compared, the pheromones that likely form the basis for species recognition are only rarely found in the androconia that are unique to either of the compared species, but rather in the basal cell brush present in all but a few species of the genus. This suggests that there may be alternative functions for the androconia in some species.

The authors are not aware of any published work on the androconia in the Afrotropical *Neptis*. An important first step would be laboratory analysis to determine whether pheromones are indeed distributed from their androconia. Field study of the mating behaviour of the *Neptis* species above might also indicate alternative functions, for example, exposure of the androconia, which are normally covered by the forewing, as a visual stimulus to the female prior to mating.

Holotype of *Neptis lugubris*

Richardson (2019) stated that the holotype of *N. lugubris* is missing. Steve Collins passed on the copious notes on the *Neptis* assembled by Torben Larsen and these contained images of the holotype annotated with “Vienna”. Subsequently Dr Sabine Gaal-Haszler, confirmed that the holotype is held in the Naturhistorisches Museum, Wien.

Etymological choices

There is growing sentiment that newly described species from countries in the Global South should not be given names honouring people in the Global North who have no connection to the taxa or their indigenous ranges (Trisos *et al.*, 2021). However, given the large number of African *Neptis* species awaiting description, we felt it appropriate to name a few species after individuals who have directly

or indirectly made this taxonomic research possible. Without their support, these species might have gone unnamed and unappreciated in biodiversity assessments for many years to come.

ACKNOWLEDGEMENTS

The revision of the *Neptis* genus in the Afrotropical region has only been possible because of the large number of specimens, from localities across the region, assembled by Steve Collins in the ABRI collection in Karen, Kenya. Steve has funded much of the collection and curation work himself as well as providing accommodation for researchers working on the collection.

Robert and Ginette Ducarme have provided the third author with many *Neptis* specimens that have augmented the series from ABRI and provided the holotype male of *Neptis ducarmei*.

Oskar Brattström is thanked for sharing his insights into the function of the androconia in *Bicyclus* butterflies and contributing to the discussion section.

Our thanks to Hitoshi Takano at the ANHRT for providing images of the paratype female of *Neptis kupe*.

David J. Lohman was supported by National Science Foundation grant DEB-1541557.

LITERATURE CITED

- AURIVILLIUS, [P.O.] C. 1894. Beiträge zur Kenntniss der Insektenfauna von Kameroun. 2. Tagfalter. *Entomologisk Tidskrift* **15**: 273–314. <http://www.biodiversitylibrary.org/item/43651>.
- AURIVILLIUS, [P.O.] C. 1895. Diagnosen neuer Tagfalter aus Africa. *Entomologische Nachrichten. Berlin* **21**: 379–382. <http://www.biodiversitylibrary.org/item/81940>.
- BACQUET, P. M. B., BRATTSTRÖM, O., WANG, H. L., ALLEN, C. E., LÖFSTEDT, C., BRAKEFIELD, P. M., & NIEBERDING C. M. 2015. Selection on male sex pheromone composition contributes to butterfly reproductive isolation. *Proceedings of the Royal Society of London B: Biological Sciences* **282**: 20142734. <http://doi.org/10.1098/rspb.2014.2734>.
- BOPPRÉ, M., & VANE-WRIGHT, R. I. 1989. Androconial systems in Danainae (Lepidoptera): Functional morphology of *Amauris*, *Danaus*, *Tirumala* and *Euploea*. *Zoological Journal of the Linnean Society* **97**: 101–133. <https://doi.org/10.1111/j.1096-3642.1989.tb00549.x>.
- BYERS, K. J. R. P., DARRAGH, K., MUSGROVE, J., ALMEIDA, D. A., GARZA, S. F., WARREN, I. A., RASTAS, P. M., KUČKA, M., CHAN, Y. F., MERRILL, R. M., SCHULZ, S., MCMILLAN, W. O., & JIGGINS, C. D. 2020. A major locus controls a biologically active pheromone component in *Heliconius melpomene*. *Evolution* **74**: 349–364. <https://doi.org/10.1111/evo.13922>.
- CAMA, B., EHLERS, S., SZCZERBOWSKI, D., THOMAS-OATES, J., JIGGINS, C. D., SCHULZ, S., MCMILLAN, W. O., & DASMAHAPATRA K. K. 2022. Exploitation of an ancestral pheromone biosynthetic pathway contributes to diversification in

- Heliconius* butterflies. Proceedings of the Royal Society B: Biological Sciences **289**: 20220474. <https://doi.org/10.1098/rspb.2022.0474>.
- CONDAMIN, M. 1966. *Bulletin de l'Institut Fondamental d'Afrique Noire (A)* **28**: 1008–1029.
- DARRAGH, K., VANJARI, S., MANN, F., GONZALEZ-ROJAS, M. F., MORRISON, C. R., SALAZAR, C., PARDO-DIAZ, C., MERRILL, R. M., MCMILLAN, W. O., SCHULZ, S. & JIGGINS, C. D. 2017. Male sex pheromone components in *Heliconius* butterflies released by the androconia affect female choice. *PeerJ* **5**: e3953. <https://doi.org/10.7717/peerj.3953>.
- GUINDON, S., DUFAYARD, J.F., LEFORT, V., ANISIMOVA, M., HORDIJK, W. & GASCUEL, O. 2010. New algorithms and methods to estimate maximum-likelihood phylogenies: Assessing the performance of PhyML 3.0. *Systematic Biology* **59**: 307–321.
- HALL, T., 1999. BioEdit: A User-Friendly Biological Sequence Alignment Editor and Analysis Program for Windows 95/98/NT. *Nucleic Acids Symposium Series*, 95–98.
- HOANG, D.T., CHERNOMOR, O., VON HAESLER, A., MINH, B.Q., VINH, L.S., 2018. UFBoot2: Improving the ultrafast bootstrap approximation. *Molecular Biology and Evolution* **35**: 518–522.
- HOLLAND, W.J., 1892. New species of *Neptis* from Africa. *Entomological News* **3**: 248–250. <http://www.biodiversitylibrary.org/bibliography/2359>.
- KALYAANAMOORTHY, S., MINH, B.Q., WONG, T.K.F., VON HAESLER, A. & JERMIIN, L.S., 2017. ModelFinder: Fast model selection for accurate phylogenetic estimates. *Nature Methods*, **14**: 587–589.
- MA, L., ZHANG, Y., LOHMAN, D. J., WAHLBERG, N., MA, F., NYLIN, S., JANZ, N., YAGO, M., ADUSE-POKU, K., PEGGIE, D., WANG, M., ZHANG, P., and WANG, H. 2020. A phylogenomic tree inferred with an inexpensive PCR-generated probe kit resolves higher-level relationships among *Neptis* butterflies (Nymphalidae: Limenitidinae). *Systematic Entomology* **45**: 924–934.
- MINH, B.Q., SCHMIDT, H.A., CHERNOMOR, O., SCHREMPF, D., WOODHAMS, M.D., VON HAESLER, A., LANFEAR, R. 2020. IQ-TREE 2: New models and efficient methods for phylogenetic inference in the genomic era. *Molecular Biology and Evolution* **37**: 1530–1534.
- NEAVE, S.A. 1904. On a large collection of Rhopalocera from the shores of the Victoria Nyanza. *Novitates Zoologicae* **11**: 323–363. <http://www.biodiversitylibrary.org/item/24181>.
- OVERLAET F.G. 1955. Exploration du Parc National de l'Upemba; Danaidae, Satyridae, Nymphalidae, Acraeidae. *Institut des Parcs Nationaux du Congo Belge* **27**: 87–98.
- PIERRE-BALTHUS C. 1978. Résultats d'élevages de *Neptis* a facies 'melicerta' en Côte d'Ivoire; description de trois nouvelles especes (Lepidoptera Nymphalidae). *Lambillionea* **78** (5–6): 33–44.
- PIERRE-BALTHUS C. & PIERRE J. 2007. Les *Neptis* africains a facies *nysiades*: apport des elevages dans la taxonomie de ce groupe (Lepidoptera, Nymphalidae). *Bulletin de la Société Entomologique de France* **112**(4): 515–528.
- REBEL, H. 1914. Wissenschaftliche Ergebnisse der Expedition R. Grauer nach Zentralafrika, Dezember 1909 bis 1911. Lepidopteren. *Annalen des (K.K.) Naturhistorischen Hofmuseums*. Wien **28**: 219–294.
- RICHARDSON, I.D. 2019. Revision of the genus *Neptis* (Lepidoptera: Nymphalidae) in the Afrotropical Region: Currently described taxa. *Metamorphosis* **30**: 69–221.
- RICHARDSON, I.D. 2020. Revision of the genus *Neptis* Fabricius, 1807 (Lepidoptera: Nymphalidae) in the Afrotropical Region, Part 2: Two new species in the Agatha group. *Metamorphosis* **31**(1): 84–93.
- RICHARDSON, I.D. 2020. Revision of the genus *Neptis* Fabricius, 1807 (Lepidoptera, Nymphalidae) in the Afrotropical Region, Part 3: A new species from Mt Mabu, Moçambique. *Metamorphosis* **31**(1): 132–138.
- SOUBRIER, J., STEEL, M., LEE, M.S.Y., SARKISSIAN, C.D., GUINDON, S., HO, S.Y.W., COOPER, A., 2012. The influence of rate heterogeneity among sites on the time dependence of molecular rates. *Molecular Biology and Evolution* **29**: 3345–3358.
- TAMURA, K., STETCHER, G., PETERSON, D., FILIPSKI, A., KUMAR, S., 2013. MEGA6: Molecular Evolutionary Genetics Analysis Version 6.0. *Molecular Biology and Evolution* **30**: 2725–2729.
- TEMPLETON, A.R., CRANDALL, K.A. & SING, C.F. 1992. A cladistic analysis of phenotypic associations with haplotypes inferred from restriction endonuclease mapping and DNA sequence data. III. Cladogram estimation. *Genetics* **132**: 619–633.
- TRIFINOPOULOS, J., NGUYEN, L.-T., VON HAESLER, A. & MINH, B.Q. 2016. W-IQ-TREE: a fast online phylogenetic tool for maximum likelihood analysis. *Nucleic Acids Research* **44**: W232–W235. <https://doi.org/10.1093/nar/gkw256>.
- ZHANG, J., KAPLI, P., PAVLIDIS, P., & STAMATAKIS, A. 2013. A general species delimitation method with applications to phylogenetic placements. *Bioinformatics* **29**: 2869–2876. <https://doi.org/10.1093/bioinformatics/btt499>.

GAZETTEER

Note: Where elevation is not specified on the specimen labels, it has been deduced using Google Earth. The gazetteer includes the estimated locality for the holotype of *N. lugubris* taken from Richardson 2019. This is an approximation based on the capture date and the route undertaken by the collector.

Locality	Country, Province	Latitude (deg°min'sec'')	Longitude (deg°min'sec'')	Elevation(m)
Biakato	DRC, Ituri	00°49' N	29°14' E	900
Ekombe	DRC, Equateur	00°24' S	18°23' E	330
Ivindo National Park	Gabon, Ogooué-Ivindo	00°30'40" N	12°48'10" E	530
Kanyambia	DRC, Nord-Kivu	00°12' S	29°12' E	2000–2200
Kanyasi	DRC, Ituri	01°35'15" N	30°13'15" E	1200
Kasugho	DRC, Nord-Kivu	00°15' S	29°15' E	1800
Kasuo	DRC, Nord-Kivu	00°14' S	29°03' E	1800–1900
Kibale	DRC, Nord Kivu	00°15' S	29°06' E	1900
Kilau	DRC, Nord-Kivu	00°11' S	29°06' E	1900–2150
Kipese	DRC, Nord-Kivu	00°14' S	29°18' E	2400
Kirima	DRC, Ituri	01°10' N	29°07' E	800–900
Kithokolo	DRC, Nord-Kivu	00°10' S	29°13' E	1900–2100
Mt. Kupe	Cameroon, South West	04°48' N	09°43' E	1000–2000
Kwokoro	DRC, Sud-Ubangi	02°40' N	19°44' E	400
Lubango	DRC, Nord-Kivu	00°19' S	29°12' E	2100–2250
Mabungu	DRC, Nord-Kivu	00°01' S	29°05' E	1100–1200
Makele	DRC, Ituri	00°56' N	29°27' E	950
Mamove	DRC, Nord-Kivu	00°01' S	29°05' E	1000
Manzumbu	DRC, Ituri	00°55' N	29°14' E	850
Mecalat	Cameroon, South	02°56' N	11°10' E	600
Otto Maber	DRC, Ituri	01°04'32" N	29°35'17" E	1050
Tabenken (Forest)	Cameroon, North West	06°41' N	10°45' E	1700–2200

ACRONYM LIST

Acronym	Meaning
ABRI	African Butterfly Research Institute
ANHRT	African Natural History Research Trust
APD	Average pairwise difference (between or within groups of barcodes)
BIN	Barcode Index Number
BOLD	Barcode of Life Data-system
COI	cytochrome c oxidase subunit 1
DNA	deoxyribonucleic acid
DRC	Democratic Republic of the Congo
fcr	forewing cell radial (mark)
ftc	forewing cell transverse (mark)
fd	forewing discal (band)
fpd	forewing post discal (band)
fsm	forewing submarginal (band)
hb	hindwing basal (band)
hd	hindwing discal (band)
hsm	hindwing submarginal (band)
K2P	Kimura two parameter
PD	Pairwise difference between two barcodes